

Global Bounds for the Error in Solutions of Linear Hyperbolic Systems due to Inaccurate Boundary Geometry

David A. Kopriva^{a,b}, Andrew R. Winters^{c,*}, Jan Nordström^{c,d}

^aDepartment of Mathematics, The Florida State University, Tallahassee, FL 32306, USA

^bComputational Science Research Center, San Diego State University, San Diego, CA, USA

^cDepartment of Mathematics, Applied Mathematics, Linköping University, 581 83 Linköping, Sweden

^dDepartment of Mathematics and Applied Mathematics University of Johannesburg P.O. Box 524, Auckland Park 2006, South Africa.

Abstract

We derive global estimates for the error in solutions of linear hyperbolic systems due to inaccurate boundary geometry. We show that the error is bounded by data and bounded in time when the solutions in the true and approximate domains are bounded. We show that boundary data evaluation errors due to the incorrect locations of the boundaries are secondary effects, whereas the primary errors are from the Jacobian and metric terms. In two space dimensions, specifically, we show that to lowest order the errors are proportional to the errors in the boundary curves *and* their derivatives. The results illustrate the importance of accurately approximating boundaries, and they should be helpful for high-order mesh generation and the design of optimization algorithms for boundary approximations.

1. Introduction

The quest to compute more accurate solutions of problems in fluid mechanics, electrodynamics, etc. has led to the development of high-order methods, such as spectral element methods or high-order summation-by-parts finite difference methods. Spectral element methods, in particular, are now mature, with a number of open source implementations available to solve complex physical problems in complex domains [1, 2, 3, 4, 5, 6, 7, 8].

As accurate as these methods can be, *the solutions are only as good as the meshes on which they are solved*, yet convergence error analysis typically overlooks errors introduced by the mesh. In almost every implementation, the boundaries of the domains on which the solutions are sought are only approximations to the true domains, especially when those boundaries are curved. Spectral element methods, for instance, approximate boundaries by high-order isoparametric polynomial orthogonal projections or interpolations of the correct boundaries. These boundary approximations introduce errors, and it has been shown that the “mesh generation error” can be larger than that produced by the solvers themselves [9].

To minimize the mesh generation errors, numerous efforts have been made to optimize boundary approximations, e.g. [10, 11, 12, 13] to cite only four, and different approaches have been used to perform these optimizations in each. In [10], three optimization procedures were presented using the Hausdorff distance, Fréchet distance, and a Taylor series estimate of the geometric error, the latter of

*Corresponding author

which minimizes a functional of the normal and tangent vectors. The paper [11] minimized an area-based disparity measure. The authors of [13] found optimal locations of interpolation nodes by minimizing a functional of the square of the distance between the true and approximate points, whereas the authors of [12] showed that an optimization of the curve parameterization that ensured that the boundary normals were correct at the interpolation nodes gave orders of magnitude improvement in the solution error over other approaches.

However, little has been done to show how the boundary approximation error translates into the solution error, except through numerical experiments. Without such knowledge, it is not clear how to choose the best approximation, so one has to resort to trial and error.

For hyperbolic initial boundary-value problems, there have been virtually no analytic studies of how the grid generation error affects the solutions. Energy estimates for the influence of boundary errors were derived in the short note [14]. The authors conclude that i) wavespeeds will be incorrect within the domain due to the fact that the eigenvalues of the system matrices will be different, ii) normals will be inaccurate, which can lead to incorrect specification of boundary conditions, iii) boundary conditions are applied at the wrong points in space, and iv) boundary data will be applied at the wrong locations. Looking at the error in the divergence due to inaccurate boundary approximation, the authors of [15] concluded that errors in the boundary normals and the transformation Jacobian affect the error.

In this paper, we go into more detail and derive global estimates for the error of linear hyperbolic systems due to inaccurate boundaries. We derive the error for the continuous problem, as the error generated by boundary approximations is actually independent of the numerical scheme used to solve the equations, and persists even when the solution approximation is fully converged. We show that the error is bounded when the solutions in the correct and inaccurate domains are bounded. From this bound, we find that the primary solution errors are due to errors in the Jacobian and metric terms. Errors due to evaluating boundary functions at the incorrect locations of the boundaries are secondary effects, being dependent on the product of small quantities. In two space dimensions, specifically, we show that to lowest order the errors are proportional to the errors in the boundary curves *and* their derivatives. The results illustrate how important it is to approximate boundaries accurately, and they should be helpful for high-order mesh generation and the design of optimization algorithms for boundary approximations.

2. Notation and Nomenclature

d	Number of space dimensions ≤ 3
Ω	Correct domain
Ω_e	Erroneous domain
\mathcal{D}	Reference domain = $[0, 1]^d$
\vec{x}	Space vector, $\vec{x} \in \mathcal{R}^d$
\tilde{x}	Contravariant space vector, $\tilde{x} \in \mathcal{D}$
\mathbf{q}	State vector
$\underline{\mathbf{A}}$	Matrix

$\underline{\mathbf{A}}^\pm$	Characteristic matrices, $\underline{\mathbf{A}}^\pm = \frac{1}{2}(\underline{\mathbf{A}} \pm \underline{\mathbf{A}})$
$\underline{\mathbf{R}}$	Reflection matrix
\cdot_e	Quantity on the erroneous domain
$\vec{\xi}$	Reference space coordinate, e.g. $\vec{\xi} = (\xi^1, \xi^2, \xi^3) = (\xi, \eta, \zeta)$
$\vec{X}(\vec{\xi})$	Correct mapping, $\vec{X} : \mathcal{D} \rightarrow \Omega$
$\vec{X}^e(\vec{\xi})$	Erroneous mapping, $\vec{X}^e : \mathcal{D} \rightarrow \Omega_e$
\vec{a}_i	i^{th} covariant basis vector, $\vec{a}_i = \vec{X}_{\xi^i}$
$J\vec{a}^i$	i^{th} volume weighted contravariant basis vector, $J\vec{a}^i = \vec{a}_j \times \vec{a}_k$, i, j, k cyclic
J	Transformation Jacobian $J = \vec{a}_i \cdot (\vec{a}_j \times \vec{a}_k)$, i, j, k cyclic
\hat{n}	Unit normal to the boundary of the reference domain
$\langle \cdot, \cdot \rangle$	\mathcal{L}^2 inner product
$\ \cdot\ _J$	Volume weighted \mathcal{L}^2 norm, $\langle J\cdot, \cdot \rangle^{\frac{1}{2}}$
\mathbf{e}	Solution error
ρ	Ratio of correct and erroneous Jacobians, J/J_e
ϵ	Error in the Jacobian, $\epsilon = J_e - J$
ε	Error in the Jacobian ratio, $\varepsilon = J/J_e - 1 = \rho - 1 = -\epsilon/(J + \epsilon)$
N	Polynomial order

3. Energy Bounds on the Correct and Erroneous Domains

We first introduce the notation and the energy method to compute the energy bounds for a symmetric, constant-coefficient linear hyperbolic system

$$\mathbf{q}_t + \nabla_x \cdot (\vec{\underline{\mathbf{A}}}\mathbf{q}) = 0, \quad (1)$$

where \mathbf{q} is the state vector of dimension N_{eq} , the number of equations, and

$$\vec{\underline{\mathbf{A}}} = \sum_{i=1}^d \underline{\mathbf{A}}_i \hat{x}_i = \underline{\mathbf{A}}_1 \hat{x} + \underline{\mathbf{A}}_2 \hat{y} + \dots \quad (2)$$

is a d -dimensional space vector of the coefficient matrices of size $N_{eq} \times N_{eq}$, with \hat{x}_i being a unit vector in the i^{th} coordinate direction. With this notation, product $\vec{\underline{\mathbf{A}}}\mathbf{q} = \sum_{i=1}^d (\underline{\mathbf{A}}_i \mathbf{q}) \hat{x}_i$ is a space vector of state vectors (a vector of fluxes, in this particular case). The dot product of $\vec{\underline{\mathbf{A}}}$ with a space vector, $\vec{n} = n_1 \hat{x} + n_2 \hat{y} + \dots$ is a matrix, $\underline{\mathbf{A}} = \sum_{i=1}^d A_i n_i$, from which it follows that the divergence defined as

$$\nabla_x \cdot (\vec{\underline{\mathbf{A}}}\mathbf{q}) = \sum_{i=1}^d \frac{\partial (\underline{\mathbf{A}}_i \mathbf{q})}{\partial x_i}, \quad (3)$$

is a state vector, see, e.g. [16].

The equations are posed on a domain Ω , which we call the “correct” domain. However the correct domain must almost always be approximated, especially when the boundaries are curved, which means that numerically one actually solves on an approximate, or “erroneous” domain Ω_e , see Fig. 1. In the forthcoming analysis, we assume that both the correct and erroneous domains can be mapped from a reference domain $\vec{\xi} \in \mathcal{D} = [0, 1]^d$ by a single *smooth* mapping $\vec{x} = \vec{X}(\vec{\xi})$ for the correct domain and

$\vec{x} = \vec{X}^e(\vec{\xi})$ for the erroneous one. We require smoothness so that derivatives of the error quantities are continuous. In practice, the mapping can be considered to refer to a whole domain, as would be used in a mapped finite difference approximation, or just a single boundary element in a mesh.

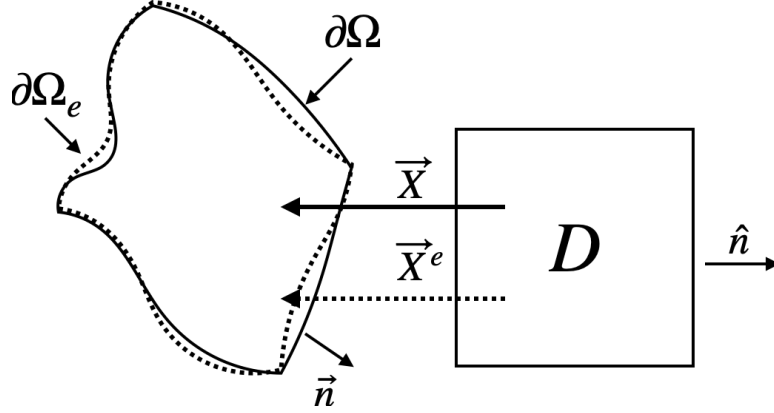


Figure 1: Diagram of the correct, Ω , erroneous, Ω_e , and reference, \mathcal{D} , domains

To complete the problem we must introduce boundary and initial conditions. We consider two types of boundary conditions here. The first sets external data, corresponding to inflow/outflow type conditions. The second sets pure reflection conditions, which correspond to wall-type boundaries. Initial conditions are specified on each domain by a function $\mathbf{q}(\vec{x}, 0) = \mathbf{q}_0(\vec{x})$.

3.1. Energy Bounds for the Correct Domain

From the transformation $\vec{x} = \vec{X}(\vec{\xi})$, we can define the covariant basis and volume weighted contravariant basis vectors

$$\vec{a}_i = \frac{\partial \vec{X}}{\partial \xi^i}, \quad J\vec{a}^i = \vec{a}_j \times \vec{a}_k, \quad i = 1, 2, 3, \quad i, j, k \text{ cyclic},$$

where, in three space dimensions, $\vec{\xi} = (\xi^1, \xi^2, \xi^3) \equiv (\xi, \eta, \zeta)$. The Jacobian of the transformation itself is $J = \vec{a}_i \cdot (\vec{a}_j \times \vec{a}_k)$, again with i, j, k cyclic.

The equations for the correct domain transform onto the reference domain as

$$J\mathbf{q}_t + \nabla_\xi \cdot (\vec{\underline{\underline{A}}}\mathbf{q}) = 0, \quad (4)$$

where the matrix components of the space vector of the contravariant coefficient matrices are $\vec{\underline{\underline{A}}}^i = J\vec{a}^i \cdot \vec{\underline{\underline{A}}}$, $i = 1, 2, 3$, so that

$$\vec{\underline{\underline{A}}} = \sum_{i=1}^d \vec{\underline{\underline{A}}}^i \hat{\xi}_i, \quad (5)$$

where $\hat{\xi}_i$ is unit coordinate vector the i^{th} coordinate direction in reference space. We assume that the correct domain is “valid” in that $J_{max} \geq J \geq J_{min} > 0$. Due to the metric identities, $\sum_{i=1}^d \frac{\partial (J\vec{a}_n^i)}{\partial \xi^i} = 0$, $n = 1, 2, \dots, d$, and the fact that $\vec{\underline{\underline{A}}}$ is constant, $\nabla_\xi \cdot \vec{\underline{\underline{A}}} = 0$, cf. [17].

The solution energy is bounded by boundary and initial data. To show this, let $\phi \in \mathcal{L}^2$ be a test function and let

$$\langle \mathbf{q}, \phi \rangle = \int_{\mathcal{D}} \mathbf{q}^T \phi d\vec{\xi} \quad (6)$$

be the \mathcal{L}^2 inner product. Multiplying (4) by ϕ^T and integrating over the domain can be written in inner product notation as

$$\langle J\mathbf{q}_t, \phi \rangle + \left\langle \nabla_\xi \cdot \left(\vec{\underline{\mathbf{A}}}\mathbf{q} \right), \phi \right\rangle = 0. \quad (7)$$

We then integrate the divergence term by parts to separate the boundary from the interior. Since the symmetric coefficient matrices are constant, and the divergence of the metric terms is zero,

$$\langle J\mathbf{q}_t, \phi \rangle + \int_{\partial\mathcal{D}} \phi^T \vec{\underline{\mathbf{A}}} \cdot \hat{n}\mathbf{q} \, dS - \left\langle \mathbf{q}, \nabla_\xi \cdot \left(\vec{\underline{\mathbf{A}}}\phi \right) \right\rangle = 0. \quad (8)$$

To obtain the energy, one replaces $\phi \leftarrow \mathbf{q}$ so that $\langle J\mathbf{q}_t, \mathbf{q} \rangle = \frac{1}{2} \frac{d}{dt} \|\mathbf{q}\|_J^2$. Let the normal coefficient matrix be defined as $\underline{\mathbf{A}} \equiv \vec{\underline{\mathbf{A}}} \cdot \hat{n}$, where \hat{n} is the outward normal to the reference domain. The volume term is converted to a surface term, for with $\underline{\mathbf{A}}$ constant and symmetric,

$$\left\langle \mathbf{q}, \nabla_\xi \cdot \left(\vec{\underline{\mathbf{A}}}\mathbf{q} \right) \right\rangle = \int_{\partial\mathcal{D}} \mathbf{q}^T \underline{\mathbf{A}}\mathbf{q} \, dS - \left\langle \nabla_\xi \cdot \left(\vec{\underline{\mathbf{A}}}\mathbf{q} \right), \mathbf{q} \right\rangle, \quad (9)$$

becomes

$$\left\langle \mathbf{q}, \nabla_\xi \cdot \left(\vec{\underline{\mathbf{A}}}\mathbf{q} \right) \right\rangle = \frac{1}{2} \int_{\partial\mathcal{D}} \mathbf{q}^T \underline{\mathbf{A}}\mathbf{q} \, dS. \quad (10)$$

Then the energy satisfies

$$\frac{d}{dt} \|\mathbf{q}\|_J^2 + \int_{\partial\mathcal{D}} \mathbf{q}^T \underline{\mathbf{A}}\mathbf{q} \, dS = 0. \quad (11)$$

Since we incorporate the two types of boundary conditions, we group the boundary into two parts, $\partial D = \partial D_g \cup \partial D_r$, where external boundary data is applied along ∂D_g , and reflection conditions are applied along ∂D_r .

Along ∂D_g , we apply characteristic boundary conditions and split the normal coefficient matrix according to its positive and negative eigenvalues as $\underline{\mathbf{A}} = \underline{\mathbf{A}}^+ + \underline{\mathbf{A}}^-$ where $\underline{\mathbf{A}}^\pm = \frac{1}{2}(\underline{\mathbf{A}} \pm |\underline{\mathbf{A}}|)$. Since the coefficient matrices are symmetric, we can write

$$\underline{\mathbf{A}} = \underline{\mathbf{P}} \underline{\mathbf{\Lambda}} \underline{\mathbf{P}}^T = \underline{\mathbf{P}} \underline{\mathbf{\Lambda}}^+ \underline{\mathbf{P}}^T + \underline{\mathbf{P}} \underline{\mathbf{\Lambda}}^- \underline{\mathbf{P}}^T \equiv \underline{\mathbf{A}}^+ + \underline{\mathbf{A}}^-, \quad (12)$$

where

$$\underline{\mathbf{\Lambda}}^+ = \begin{bmatrix} \bar{\underline{\mathbf{\Lambda}}}^+ & \mathbf{0} \\ \mathbf{0} & \mathbf{0} \end{bmatrix}, \quad \underline{\mathbf{\Lambda}}^- = \begin{bmatrix} \mathbf{0} & \mathbf{0} \\ \mathbf{0} & \bar{\underline{\mathbf{\Lambda}}}^- \end{bmatrix}. \quad (13)$$

The matrices $\bar{\underline{\mathbf{\Lambda}}}^\pm$ contain the positive and negative eigenvalues of $\underline{\mathbf{A}}$. (We assume no zero eigenvalues, but if they are present they do not affect the results.) Then

$$\int_{\partial\mathcal{D}_g} \mathbf{q}^T \underline{\mathbf{A}}\mathbf{q} \, dS = \int_{\partial\mathcal{D}_g} \mathbf{q}^T \underline{\mathbf{A}}^+\mathbf{q} \, dS - \int_{\partial\mathcal{D}_g} \mathbf{q}^T |\underline{\mathbf{A}}^-|\mathbf{q} \, dS. \quad (14)$$

Specifying external data is equivalent to replacing $\mathbf{q} = \mathbf{g}(\vec{x}, t)$ in the $|\underline{\mathbf{A}}^-|$ term in (14), where \mathbf{g} is boundary data,

$$\int_{\partial\mathcal{D}_g} \mathbf{q}^T \underline{\mathbf{A}}\mathbf{q} \, dS \leftarrow \int_{\partial\mathcal{D}_g} \mathbf{q}^T \underline{\mathbf{A}}^+\mathbf{q} \, dS - \int_{\partial\mathcal{D}_g} \mathbf{g}^T \left(\vec{X} \left(\vec{\xi} \right), t \right) |\underline{\mathbf{A}}^-| \mathbf{g} \left(\vec{X} \left(\vec{\xi} \right), t \right) \, dS, \quad (15)$$

see [18].

The second boundary condition along $\partial\mathcal{D}_r$ represents reflection, and includes wall-type conditions. Here, characteristic boundary data is also used to determine the boundary terms, writing

$$\mathbf{q}^T \underline{\Lambda} \mathbf{q} = \mathbf{q}^T \underline{\mathbf{P}} \underline{\Lambda} (\underline{\mathbf{P}}^T \mathbf{q}) \equiv \mathbf{w}^T \underline{\Lambda} \mathbf{w} = \begin{bmatrix} \mathbf{w}^+ \\ \mathbf{w}^- \end{bmatrix}^T \begin{bmatrix} \underline{\Lambda}^+ & \underline{\mathbf{0}} \\ \underline{\mathbf{0}} & \underline{\Lambda}^- \end{bmatrix} \begin{bmatrix} \mathbf{w}^+ \\ \mathbf{w}^- \end{bmatrix}, \quad (16)$$

where $\mathbf{w} = \underline{\mathbf{P}}^T \mathbf{q}$ and \mathbf{w}^\pm are the characteristic variables grouped according to the positive and negative eigenvalues of $\underline{\Lambda}$.

The general form of reflection boundary conditions without sources are of the form

$$\mathbf{w}^- = \underline{\bar{\mathbf{R}}} \mathbf{w}^+, \quad (17)$$

where $\underline{\bar{\mathbf{R}}}$ is the reflection matrix. Then, with the boundary condition, (17), the reflected state is

$$\mathbf{w}_R = \begin{bmatrix} \underline{\mathbf{I}} & \underline{\mathbf{0}} \\ \underline{\bar{\mathbf{R}}} & \underline{\mathbf{0}} \end{bmatrix} \mathbf{w} \equiv \underline{\mathbf{R}} \mathbf{w}. \quad (18)$$

Inserting the boundary condition (18) into the boundary integrand,

$$\mathbf{q}^T \underline{\Lambda} \mathbf{q} \leftarrow \mathbf{w}^T \underline{\Lambda}^+ \mathbf{w} + \mathbf{w}^T \underline{\mathbf{R}}^T \underline{\Lambda}^- \underline{\mathbf{R}} \mathbf{w} = \mathbf{q}^T [\underline{\mathbf{P}} (\underline{\Lambda}^+ + \underline{\mathbf{R}}^T \underline{\Lambda}^- \underline{\mathbf{R}}) \underline{\mathbf{P}}^T] \mathbf{q} \quad (19)$$

along reflection boundaries, so the boundary term is non-negative if the reflection matrix $\underline{\mathbf{R}}$ satisfies

$$\underline{\Lambda}^+ + \underline{\mathbf{R}}^T \underline{\Lambda}^- \underline{\mathbf{R}} \geq 0. \quad (20)$$

In this paper we will assume that the reflection matrix is specified so that (20) is true.

Remark 1. Setting $\underline{\mathbf{R}} = 0$ is equivalent to setting trivial boundary data, $\mathbf{g} = 0$.

Gathering the results,

$$\begin{aligned} \frac{d}{dt} \|\mathbf{q}\|_J^2 + \int_{\partial\mathcal{D}_r} \mathbf{q}^T [\underline{\mathbf{P}} (\underline{\Lambda}^+ + \underline{\mathbf{R}}^T \underline{\Lambda}^- \underline{\mathbf{R}}) \underline{\mathbf{P}}^T] \mathbf{q} \, dS + \int_{\partial\mathcal{D}_g} \mathbf{q}^T \underline{\Lambda}^+ \mathbf{q} \, dS \\ = \int_{\partial\mathcal{D}_g} \mathbf{g}^T (\vec{X}(\vec{\xi}), t) |\underline{\Lambda}^-| \mathbf{g} (\vec{X}(\vec{\xi}), t) \, dS. \end{aligned} \quad (21)$$

The boundary terms on the left of (21) are dissipative, so, after we integrate in time and apply the initial condition $\mathbf{q}(\vec{x}, 0) = \mathbf{q}_0(\vec{x})$,

$$\|\mathbf{q}(t)\|_J^2 \leq \left\| \mathbf{q}_0(\vec{X}(\vec{\xi})) \right\|_J^2 + \int_0^t \int_{\partial\mathcal{D}_g} \mathbf{g}^T (\vec{X}(\vec{\xi}), t) |\underline{\Lambda}^-| \mathbf{g} (\vec{X}(\vec{\xi}), t) \, dS dt. \quad (22)$$

Thus, the energy is bounded by initial and boundary data.

Remark 2. The case

$$\underline{\Lambda}^+ + \underline{\mathbf{R}}^T \underline{\Lambda}^- \underline{\mathbf{R}} = 0 \quad (23)$$

produces no loss or growth of energy. For instance if $\partial\mathcal{D}_g = \emptyset$, then

$$\|\mathbf{q}(t)\|_J = \left\| \mathbf{q}_0(\vec{X}(\vec{\xi})) \right\|_J, \quad (24)$$

so (23) corresponds to a perfectly reflecting boundary condition.

3.2. Energy Bounds for the Erroneous Domain

Now we assume that errors are introduced along the boundary of the correct domain, e.g. due to approximating boundary curves and surfaces, creating the “erroneous” domain, Ω_e . In that case, there is a different mapping, $\vec{x} = \vec{X}^e(\vec{\xi})$ from the reference domain to the erroneous domain. We assume that the erroneous domain is still valid in that $J_{e,max} \geq J_e \geq J_{e,min} > 0$. For the erroneous problem, let $\vec{\underline{\mathbf{B}}}^i = J\vec{a}_e^i \cdot \vec{\underline{\mathbf{A}}}$ so that the erroneous solution, \mathbf{v} , satisfies

$$J_e \mathbf{v}_t + \nabla_{\xi} \cdot (\vec{\underline{\mathbf{B}}}\mathbf{v}) = 0. \quad (25)$$

It follows also that $\nabla_{\xi} \cdot \vec{\underline{\mathbf{B}}} = 0$.

Following the same steps as for the solution on the correct domain, the solution on the erroneous domain is also bounded by data if boundary data is specified and exists,

$$\|\mathbf{v}(t)\|_{J_e}^2 \leq \|\mathbf{q}_0(\vec{X}^e(\vec{\xi}))\|_{J_e}^2 + \int_0^t \int_{\partial D_g} \mathbf{g}^T(\vec{X}^e(\vec{\xi}), t) |\underline{\mathbf{B}}^-| \mathbf{g}(\vec{X}^e(\vec{\xi}), t) \, dS, \quad (26)$$

provided that any reflection matrix $\underline{\mathbf{R}}_e$ satisfies

$$\underline{\Lambda}_e^+ + \underline{\mathbf{R}}_e^T \underline{\Lambda}_e^- \underline{\mathbf{R}}_e \geq 0. \quad (27)$$

Several technical considerations should be noted for (26) to be valid. First, the boundary values and initial conditions must exist on both domains, that is, the bounds require that the boundary conditions are defined on both $\partial\Omega$ and $\partial\Omega_e$, and initial conditions are defined on both Ω and Ω_e . This can be either trivial, e.g. constant inflow conditions, or not, and might require some sort of extension of the conditions. The extension itself may be completely erroneous. In fact, \mathbf{g} may not even be defined for those values of \vec{X}^e .

Example 1. Suppose $\min_x \Omega = 0$ and $\mathbf{g}(x) = \sqrt{x}$. Then if Ω_e is a high order polynomial interpolation of Ω , oscillations in the polynomial will produce sections where $x < 0$, and \mathbf{g} will not exist at those points. The same holds true with regards to the initial condition, \mathbf{q}_0 .

Next, the boundary segmentations, ∂D_g and ∂D_r do not have to be the same, since the parametrizations can differ so that at a particular value of $\vec{\xi}$ in one domain may have specified conditions while the other has reflections. To simplify the analysis, we require that the boundary segmentations be the same for both domains. In practice, this is not a concern since domains (and elements) are usually defined so that only one boundary condition is applied to any parametrized segment of the boundary, e.g. one side of an element.

Finally, the energy may also not be bounded if the exact reflection conditions $\underline{\mathbf{R}}$ are applied on the erroneous boundary. For $\partial D_g = \emptyset$ with $\underline{\mathbf{R}}_e = \underline{\mathbf{R}}$, the energy method produces

$$\frac{d}{dt} \|\mathbf{v}\|_J^2 + \int_{\partial D} \mathbf{v}^T [\underline{\mathbf{P}}_e (\underline{\Lambda}_e^+ + \underline{\mathbf{R}}^T \underline{\Lambda}_e^- \underline{\mathbf{R}}) \underline{\mathbf{P}}_e^T] \mathbf{v} \, dS = 0, \quad (28)$$

but only if the number of positive and negative eigenvalues do not differ between the correct and erroneous domains. (These can differ depending on the differences in the normals.) If they do, then the reflection matrix doesn't have the correct dimensions and the problem is ill-posed. Even so, if we write $\underline{\Lambda}_e^+ = \underline{\Lambda}^+ + \Delta \underline{\Lambda}^+$, etc., then

$$\underline{\Lambda}_e^+ + \underline{\mathbf{R}}^T \underline{\Lambda}_e^- \underline{\mathbf{R}} = (\underline{\Lambda}^+ + \underline{\mathbf{R}}^T \underline{\Lambda}^- \underline{\mathbf{R}}) + (\Delta \underline{\Lambda}^+ + \underline{\mathbf{R}}^T \Delta \underline{\Lambda}^- \underline{\mathbf{R}}). \quad (29)$$

Therefore the energy in (28) is only bounded if

$$(\Delta\Lambda^+ + \mathbf{R}^T \Delta\Lambda^- \mathbf{R}) + (\Lambda^+ + \mathbf{R}^T \Lambda^- \mathbf{R}) \geq 0. \quad (30)$$

If, for instance, perfect reflection conditions are specified for the correct domain, then boundedness requires that

$$(\Delta\Lambda^+ + \mathbf{R}^T \Delta\Lambda^- \mathbf{R}) \geq 0, \quad (31)$$

which, depending on the boundary errors, does not have to hold. To ensure that the erroneous problem is energy bounded, we require that the reflection matrix, R_e , satisfies (27). In practice, i.e. in numerical simulations, a reflection condition is usually implemented using the available (erroneous) geometry, thus ensuring (27).

Remark 3. *We see, then, that a well-posed problem on the correct domain does not necessarily imply well-posedness on the erroneous domain. But we will not consider the “worst case” scenarios here. Instead, we require the more likely situations where conditions on the initial and boundary values are defined so that the problems on both domains are well-posed.*

In addition to existing on both domains, we will also require that the boundary and initial data are smooth. For example, the initial condition is $\mathbf{q}_0(\vec{x})$, and that it is defined on both the correct and erroneous domains. Then by the mean value theorem,

$$\mathbf{e}(\vec{\xi}, 0) \equiv \mathbf{q}_0(\vec{X}^e(\vec{\xi})) - \mathbf{q}_0(\vec{X}(\vec{\xi})) = \nabla_x \mathbf{q}_0(\vec{\nu}) \cdot (\vec{X}^e(\vec{\xi}) - \vec{X}(\vec{\xi})) \quad (32)$$

for some $\vec{\nu}$. For the initial error to depend continuously on the error in the mappings, the initial condition must be Lipschitz continuous. So, in addition to existence of boundary and initial data on both domains, we will require in the following that the error in the data is continuous with respect to the domain error and that all data have continuous and bounded first derivatives. What happens when jump discontinuities, e.g. shocks, are present is certainly important, but will not be considered at this time.

4. The Error Equation

The goal is to find how the erroneous solution, \mathbf{v} , and the correct solution, \mathbf{q} , differ. It is not easy to decide how to measure that error. If one attempts to measure it in physical space, then it is *undefined* in the regions where the two domains do not overlap. (See Fig. 1.) On the other hand, the error is defined at all points in reference space. Although defining the error in reference space has the disadvantage that the difference between two values in reference space corresponds to the error at different physical space locations except in the limit as $\Omega_e \rightarrow \Omega$, it continuously converges to zero in that limit. For these reasons, we measure the error in reference space.

To that end, we multiply (25) by the ratio of the Jacobians, $\rho \equiv J/J_e > 0$, to get

$$J\mathbf{v}_t + \rho \nabla_\xi \cdot (\vec{\mathbf{B}}\mathbf{v}) = 0 \quad (33)$$

for the erroneous solution. We define the error equation by the difference between (33) and (4),

$$J(\mathbf{v} - \mathbf{q})_t + \rho \nabla_\xi \cdot (\vec{\mathbf{B}}\mathbf{v}) - \nabla_\xi \cdot (\vec{\mathbf{A}}\mathbf{q}) = 0. \quad (34)$$

For any $\mathcal{L}^2 \cap C^0$ test function, ϕ , remembering that we are requiring extra smoothness in the data,

$$\langle J(\mathbf{v} - \mathbf{q})_t, \phi \rangle + \langle \rho \nabla_\xi \cdot (\vec{\mathbf{B}}\mathbf{v}), \phi \rangle - \langle \nabla_\xi \cdot (\vec{\mathbf{A}}\mathbf{q}), \phi \rangle = 0. \quad (35)$$

To separate erroneous from correct quantities, we define the error matrix $\vec{\mathbf{E}}$ through

$$\vec{\mathbf{B}} = \vec{\mathbf{A}} + \vec{\mathbf{E}}. \quad (36)$$

Since the coefficient matrix of the original problem is constant, the error matrix

$$\vec{\mathbf{E}} = \sum_{i=1}^d \{ J\vec{a}_e^i - J\vec{a}^i \} \cdot \vec{\mathbf{A}}\hat{\xi}^i \quad (37)$$

depends only on the error in the metric terms. Note in particular that $\nabla_\xi \cdot \vec{\mathbf{E}} = 0$ since in both cases the volume weighted contravariant basis vectors satisfy the metric identities.

Let us also define the Jacobian error, ε , through $\rho = 1 + \varepsilon = 1 + \left(\frac{J}{J_e} - 1\right)$. Note that for valid domains, $\rho > 0$, so $\varepsilon > -1$. In terms of the error matrix and Jacobian errors,

$$\begin{aligned} \langle \rho \nabla_\xi \cdot (\vec{\mathbf{B}}\mathbf{v}), \phi \rangle &= \langle (1 + \varepsilon) \nabla_\xi \cdot (\vec{\mathbf{A}} + \vec{\mathbf{E}})\mathbf{v}, \phi \rangle \\ &= \langle \nabla_\xi \cdot (\vec{\mathbf{A}}\mathbf{v}), \phi \rangle + \langle \varepsilon \nabla_\xi \cdot (\vec{\mathbf{A}}\mathbf{v}), \phi \rangle + \langle (1 + \varepsilon) \nabla_\xi \cdot (\vec{\mathbf{E}}\mathbf{v}), \phi \rangle. \end{aligned} \quad (38)$$

Remark 4. Note that the second and third terms on the right of (38) are expected to be small for small deformations of the domain, and the product of ε and $\vec{\mathbf{E}}$ will be secondary since $\varepsilon \nabla_\xi \cdot (\vec{\mathbf{E}}\mathbf{v}) = (\varepsilon \vec{\mathbf{E}}) \cdot \nabla_\xi \mathbf{v}$, since it includes the product of two small quantities.

Substituting the formulation (38), the error equation (35) becomes

$$\langle J(\mathbf{v} - \mathbf{q})_t, \phi \rangle + \langle \nabla_\xi \cdot (\vec{\mathbf{A}}(\mathbf{v} - \mathbf{q})), \phi \rangle + \langle (1 + \varepsilon) \nabla_\xi \cdot (\vec{\mathbf{E}}\mathbf{v}), \phi \rangle + \langle \varepsilon \nabla_\xi \cdot (\vec{\mathbf{A}}\mathbf{v}), \phi \rangle = 0. \quad (39)$$

Let the error be $\mathbf{e} \equiv \mathbf{v} - \mathbf{q}$, which, again, is defined on the reference domain. Then $\mathbf{v} = \mathbf{q} + \mathbf{e}$ and

$$\begin{aligned} \langle J\mathbf{e}_t, \phi \rangle + \langle \nabla_\xi \cdot (\vec{\mathbf{A}}\mathbf{e}), \phi \rangle + \langle (1 + \varepsilon) \nabla_\xi \cdot (\vec{\mathbf{E}}\mathbf{e}), \phi \rangle + \langle \varepsilon \nabla_\xi \cdot (\vec{\mathbf{A}}\mathbf{e}), \phi \rangle \\ + \langle (1 + \varepsilon) \nabla_\xi \cdot (\vec{\mathbf{E}}\mathbf{q}), \phi \rangle + \langle \varepsilon \nabla_\xi \cdot (\vec{\mathbf{A}}\mathbf{q}), \phi \rangle = 0 \end{aligned} \quad (40)$$

is the error equation. When we set $\phi = \mathbf{e}$, we get an equation for the energy of the error,

$$\begin{aligned} \frac{1}{2} \frac{d}{dt} \|\mathbf{e}\|_J^2 + \langle \nabla_\xi \cdot (\vec{\mathbf{A}}\mathbf{e}), \mathbf{e} \rangle + \langle (1 + \varepsilon) \nabla_\xi \cdot (\vec{\mathbf{E}}\mathbf{e}), \mathbf{e} \rangle + \langle \varepsilon \nabla_\xi \cdot (\vec{\mathbf{A}}\mathbf{e}), \mathbf{e} \rangle \\ + \langle (1 + \varepsilon) \nabla_\xi \cdot (\vec{\mathbf{E}}\mathbf{q}), \mathbf{e} \rangle + \langle \varepsilon \nabla_\xi \cdot (\vec{\mathbf{A}}\mathbf{q}), \mathbf{e} \rangle = 0. \end{aligned} \quad (41)$$

Using integration by parts, c.f. (10),

$$\langle \nabla_\xi \cdot (\vec{\mathbf{A}}\mathbf{e}), \mathbf{e} \rangle = \frac{1}{2} \int_{\partial\mathcal{D}} \mathbf{e}^T (\vec{\mathbf{A}} \cdot \hat{\mathbf{n}}) \mathbf{e} \, dS, \quad (42)$$

where, again, $\hat{\mathbf{n}}$ is the unit outward normal on the reference domain. Next,

$$\langle \varepsilon \nabla_\xi \cdot (\vec{\mathbf{A}}\mathbf{e}), \mathbf{e} \rangle = \frac{1}{2} \int_{\partial\mathcal{D}} \varepsilon \mathbf{e}^T (\vec{\mathbf{A}} \cdot \hat{\mathbf{n}}) \mathbf{e} \, dS - \frac{1}{2} \langle \mathbf{e}, (\vec{\mathbf{A}} \cdot \nabla_\xi \varepsilon) \mathbf{e} \rangle, \quad (43)$$

so this is like the previous term but with an extra volume term due to the gradient of ε . Similarly,

$$\langle \rho \nabla_\xi \cdot (\vec{\mathbf{E}}\mathbf{e}), \mathbf{e} \rangle = \frac{1}{2} \int_{\partial\mathcal{D}} \rho \mathbf{e}^T (\vec{\mathbf{E}} \cdot \hat{\mathbf{n}}) \mathbf{e} \, dS - \frac{1}{2} \langle \mathbf{e}, (\vec{\mathbf{E}} \cdot \nabla_\xi \rho) \mathbf{e} \rangle. \quad (44)$$

We put everything so far together, use the fact that $\rho = 1 + \varepsilon$, $\nabla_\xi \rho = \nabla_\xi \varepsilon$, and gather the boundary terms, to get

$$\begin{aligned} \frac{1}{2} \frac{d}{dt} \|\mathbf{e}\|_J^2 + \frac{1}{2} \int_{\partial \mathcal{D}} (1 + \varepsilon) \mathbf{e}^T \left\{ \left(\vec{\underline{\mathbf{A}}} \cdot \hat{\mathbf{n}} \right) + \left(\vec{\underline{\mathbf{E}}} \cdot \hat{\mathbf{n}} \right) \right\} \mathbf{e} \, dS = \\ \frac{1}{2} \left\langle \mathbf{e}, \left(\vec{\underline{\mathbf{E}}} \cdot \nabla_\xi \varepsilon \right) \mathbf{e} \right\rangle + \frac{1}{2} \left\langle \mathbf{e}, \left(\vec{\underline{\mathbf{A}}} \cdot \nabla_\xi \varepsilon \right) \mathbf{e} \right\rangle - \left\langle (1 + \varepsilon) \nabla_\xi \cdot \left(\vec{\underline{\mathbf{E}}} \mathbf{q} \right), \mathbf{e} \right\rangle - \left\langle \varepsilon \nabla_\xi \cdot \left(\vec{\underline{\mathbf{A}}} \mathbf{q} \right), \mathbf{e} \right\rangle. \end{aligned} \quad (45)$$

To get a bound on the error, boundary conditions must be applied to (45). Again, we will consider both externally specified data and reflection boundary conditions.

For externally specified data, the error on ∂D_g ,

$$\int_{\partial \mathcal{D}} (1 + \varepsilon) \mathbf{e}^T \left\{ \left(\vec{\underline{\mathbf{A}}} \cdot \hat{\mathbf{n}} \right) + \left(\vec{\underline{\mathbf{E}}} \cdot \hat{\mathbf{n}} \right) \right\} \mathbf{e} \, dS = \int_{\partial \mathcal{D}} (1 + \varepsilon) \mathbf{e}^T \underline{\mathbf{B}} \mathbf{e} \, dS,$$

where $\underline{\mathbf{B}} = \vec{\underline{\mathbf{B}}} \cdot \hat{\mathbf{n}} = \vec{\underline{\mathbf{A}}} \cdot \hat{\mathbf{n}} + \vec{\underline{\mathbf{E}}} \cdot \hat{\mathbf{n}} = \underline{\mathbf{A}} + \underline{\mathbf{E}}$. To specify characteristic boundary conditions with external data, one splits the matrix $\underline{\mathbf{B}}$ according to its eigenvalues to represent outgoing and incoming waves, for which the latter is specified by data [18]. That splitting can be done here in at least three ways, see Appendix A. We will use the splitting on the right hand side of (A.4) since we can use it to relate $\underline{\mathbf{E}}^\pm$ to the boundary errors.

When we split the boundary integrals according to the right side of (A.4),

$$\int_{\partial \mathcal{D}_g} (1 + \varepsilon) \mathbf{e}^T \underline{\mathbf{B}} \mathbf{e} \, dS \leftarrow \int_{\partial \mathcal{D}_g} (1 + \varepsilon) \mathbf{e}^T (\underline{\mathbf{A}}^+ + \underline{\mathbf{E}}^+) \mathbf{e} \, dS - \int_{\partial \mathcal{D}_g} (1 + \varepsilon) \mathbf{e}_g^T (|\underline{\mathbf{A}}^-| + |\underline{\mathbf{E}}^-|) \mathbf{e}_g \, dS. \quad (46)$$

Specified boundary data is given by external states $\mathbf{g} = \mathbf{g}(\vec{x}, t)$ applied to the incoming waves. We have two ways to specify the boundary data on the erroneous domain leading to the boundary error \mathbf{e}_g :

- Evaluate the boundary data at the erroneous location, $\mathbf{g}(\vec{X}^e(\vec{\xi}), t)$.

This is what one must do when the mesh generator, e.g. HOHQMesh [19], HOPR [20], provides only an approximation to the boundary. This situation is where a boundary is defined by an interpolant only in terms of a set of points, and the exact “truth” boundary is never actually known by a solver.

- Evaluate the data at the correct location, $\mathbf{g}(\vec{X}(\vec{\xi}), t)$.

To evaluate at the correct location, the exact boundary must be supplied along with the mesh. In this case the boundary error, \mathbf{e}_g , is zero and the last term in (46) vanishes.

In the first case, error is injected at the boundary of the reference domain

$$\mathbf{e}_g = \mathbf{g}(\vec{X}^e(\vec{\xi}), t) - \mathbf{g}(\vec{X}(\vec{\xi}), t) \quad \vec{\xi} \in \partial D_g. \quad (47)$$

For smooth boundary data, the mean value theorem allows the error to be written in terms of the boundary location error $\Delta \vec{X}$ as

$$\mathbf{e}_g = \nabla_x \mathbf{g}(\vec{\nu}, t) \cdot \left(\vec{X}^e(\vec{\xi}) - \vec{X}(\vec{\xi}) \right) = \nabla_x \mathbf{g} \cdot \Delta \vec{X}(\vec{\xi}) \quad (48)$$

for some $\vec{\nu}$. Therefore, characteristic boundary terms in (46) become

$$\int_{\partial \mathcal{D}_g} (1 + \varepsilon) \mathbf{e}^T \underline{\mathbf{B}} \mathbf{e} \, dS \leftarrow \int_{\partial \mathcal{D}_g} (1 + \varepsilon) \mathbf{e}^T (\underline{\mathbf{A}}^+ + \underline{\mathbf{E}}^+) \mathbf{e} \, dS - \int_{\partial \mathcal{D}_g} (1 + \varepsilon) \Delta \vec{X}^T \cdot \nabla_x \mathbf{g}^T (|\underline{\mathbf{A}}^-| + |\underline{\mathbf{E}}^-|) \nabla_x \mathbf{g} \cdot \Delta \vec{X} \, dS. \quad (49)$$

For reflection boundaries, we replace the reflected error in the boundary term as

$$\int_{\partial\mathcal{D}_r} (1 + \varepsilon) \mathbf{e}^T \underline{\mathbf{B}} \mathbf{e} \, dS \leftarrow \int_{\partial\mathcal{D}_r} (1 + \varepsilon) \mathbf{e}^T \underline{\mathbf{B}}^+ \mathbf{e} \, dS + \int_{\partial\mathcal{D}_r} (1 + \varepsilon) \mathbf{e}_r^T \underline{\mathbf{B}}^- \mathbf{e}_r \, dS. \quad (50)$$

Let us define $\mathbf{W} = \underline{\mathbf{P}}_e^T \mathbf{e}$ to be the characteristic decomposition of the error with respect to the erroneous domain. Then

$$\int_{\partial\mathcal{D}_r} (1 + \varepsilon) [\mathbf{e}^T \underline{\mathbf{B}}^+ \mathbf{e} + \mathbf{e}_r^T \underline{\mathbf{B}}^- \mathbf{e}_r] \, dS = \int_{\partial\mathcal{D}_r} (1 + \varepsilon) [\mathbf{W}^T \underline{\Lambda}_e^+ \mathbf{W} + \mathbf{W}^T \underline{\Lambda}_e^- \mathbf{W}] \, dS. \quad (51)$$

To get the reflected error, we use the reflection matrix with respect to the erroneous domain and replace the characteristic variables in the $\underline{\Lambda}_e^-$ term with

$$\mathbf{W}_r = \underline{\mathbf{R}}_e \mathbf{W} = \underline{\mathbf{R}}_e \underline{\mathbf{P}}_e^T \mathbf{e}. \quad (52)$$

So

$$\begin{aligned} \int_{\partial\mathcal{D}_r} (1 + \varepsilon) [\mathbf{W}^T \underline{\Lambda}_e^+ \mathbf{W} + \mathbf{W}_r^T \underline{\Lambda}_e^- \mathbf{W}_r] \, dS &= \int_{\partial\mathcal{D}_r} (1 + \varepsilon) [\mathbf{W}^T \underline{\Lambda}_e^+ \mathbf{W} + \mathbf{W}^T \underline{\mathbf{R}}_e^T \underline{\Lambda}_e^- \underline{\mathbf{R}}_e \mathbf{W}] \, dS \\ &= \int_{\partial\mathcal{D}_r} (1 + \varepsilon) \mathbf{W}^T [\underline{\Lambda}_e^+ + \underline{\mathbf{R}}_e^T \underline{\Lambda}_e^- \underline{\mathbf{R}}_e] \mathbf{W} \, dS \geq 0, \end{aligned} \quad (53)$$

when the reflection matrix on the erroneous domain is chosen properly as in (27).

When the boundary data is evaluated at the correct point, the error injected along the boundary is zero, so the last term in (49) vanishes. To distinguish between the two cases, we introduce a parameter γ with

$$\gamma = \begin{cases} 1 & \text{evaluate along erroneous boundary} \\ 0 & \text{evaluate along correct boundary} \end{cases}. \quad (54)$$

Then accounting for the boundary errors, we have the final form of the error energy equation,

$$\begin{aligned} \frac{1}{2} \frac{d}{dt} \|\mathbf{e}\|_J^2 + \frac{1}{2} \int_{\partial\mathcal{D}_g} (1 + \varepsilon) \mathbf{e}^T (\underline{\mathbf{A}}^+ + \underline{\mathbf{E}}^+) \mathbf{e} \, dS + \frac{1}{2} \int_{\partial\mathcal{D}_r} (1 + \varepsilon) \mathbf{e}^T \underline{\mathbf{P}}_e^T [\underline{\Lambda}_e^+ + \underline{\mathbf{R}}_e^T \underline{\Lambda}_e^- \underline{\mathbf{R}}_e] \underline{\mathbf{P}}_e \mathbf{e} \, dS \\ = \frac{\gamma}{2} \int_{\partial\mathcal{D}_g} (1 + \varepsilon) \Delta \vec{X}^T \cdot \nabla_x \mathbf{g}^T (|\underline{\mathbf{A}}^-| + |\underline{\mathbf{E}}^-|) \nabla_x \mathbf{g} \cdot \Delta \vec{X} \, dS \\ + \frac{1}{2} \left\langle \mathbf{e}, \left(\vec{\underline{\mathbf{E}}} \cdot \nabla_\xi \varepsilon \right) \mathbf{e} \right\rangle + \frac{1}{2} \left\langle \mathbf{e}, \left(\vec{\underline{\mathbf{A}}} \cdot \nabla_\xi \varepsilon \right) \mathbf{e} \right\rangle \\ - \left\langle (1 + \varepsilon) \nabla_\xi \cdot \left(\vec{\underline{\mathbf{E}}} \mathbf{q} \right), \mathbf{e} \right\rangle - \left\langle \varepsilon \nabla_\xi \cdot \left(\vec{\underline{\mathbf{A}}} \mathbf{q} \right), \mathbf{e} \right\rangle. \end{aligned} \quad (55)$$

To keep track of the numerous terms, we write (55) in terms of the dissipation, D , boundary errors, BG , and volume errors, V_1, \dots, V_4 , as

$$\|\mathbf{e}\|_J \frac{d}{dt} \|\mathbf{e}\|_J + D = \gamma BG + V_1 + V_2 + V_3 + V_4, \quad (56)$$

where

$$\begin{aligned} D &= \frac{1}{2} \int_{\partial\mathcal{D}_g} (1 + \varepsilon) \mathbf{e}^T \underline{\mathbf{B}}^+ \mathbf{e} \, dS + \frac{1}{2} \int_{\partial\mathcal{D}_r} (1 + \varepsilon) \mathbf{e}^T \underline{\mathbf{P}}_e^T [\underline{\Lambda}_e^+ + \underline{\mathbf{R}}_e^T \underline{\Lambda}_e^- \underline{\mathbf{R}}_e] \underline{\mathbf{P}}_e \mathbf{e} \, dS \geq 0 \\ BG &= \frac{1}{2} \int_{\partial\mathcal{D}_g} (1 + \varepsilon) \Delta \vec{X}^T \cdot \nabla_x \mathbf{g}^T (|\underline{\mathbf{A}}^-| + |\underline{\mathbf{E}}^-|) \nabla_x \mathbf{g} \cdot \Delta \vec{X} \, dS \\ V_1 &= \frac{1}{2} \left\langle \mathbf{e}, \left(\vec{\underline{\mathbf{E}}} \cdot \nabla_\xi \varepsilon \right) \mathbf{e} \right\rangle, \quad V_2 = \frac{1}{2} \left\langle \mathbf{e}, \left(\vec{\underline{\mathbf{A}}} \cdot \nabla_\xi \varepsilon \right) \mathbf{e} \right\rangle, \\ V_3 &= - \left\langle (1 + \varepsilon) \nabla_\xi \cdot \left(\vec{\underline{\mathbf{E}}} \mathbf{q} \right), \mathbf{e} \right\rangle, \quad V_4 = - \left\langle \varepsilon \nabla_\xi \cdot \left(\vec{\underline{\mathbf{A}}} \mathbf{q} \right), \mathbf{e} \right\rangle. \end{aligned} \quad (57)$$

Remark 5. Equations (55) and (56) show that that even if the boundary data is computed at the correct point ($\gamma = 0$), there are still errors due to errors in the metric terms and Jacobian. It is not enough just to compute the boundary condition values correctly.

5. Error Bounds

Eqns. (22) and (26) show that the correct and erroneous solutions are each bounded, from which it follows that the error is also bounded:

Theorem 1. *The error $\|\mathbf{v} - \mathbf{q}\|_J$ is bounded by data.*

Proof. By the triangle inequality,

$$\|\mathbf{v} - \mathbf{q}\|_J \leq \|\mathbf{v}\|_J + \|\mathbf{q}\|_J. \quad (58)$$

The norm of the correct solution is bounded in (22). To get the required bound for the erroneous solution,

$$\|\mathbf{v}\|_J = \int_{\mathcal{D}} J \mathbf{v}^T \mathbf{v} d\xi = \int_{\mathcal{D}} \left(\frac{J}{J_e} \right) J_e \mathbf{v}^T \mathbf{v} d\xi = \int_{\mathcal{D}} \rho J_e \mathbf{v}^T \mathbf{v} d\xi \leq \|\rho\|_{\infty} \|\mathbf{v}\|_{J_e}. \quad (59)$$

Therefore,

$$\|\mathbf{e}\|_J \leq \|\rho\|_{\infty} \|\mathbf{v}\|_{J_e} + \|\mathbf{q}\|_J. \quad (60)$$

The ratio of Jacobians, ρ , is bounded when the domains are valid, that is, $\rho \leq J_{max}/J_{e,min}$, where $J_{e,min} > 0$. Lastly, $\|\mathbf{v}\|_{J_e}$ and $\|\mathbf{q}\|_J$ are each bounded by data through (22) and (26). \square

Actually, we want to know how the error depends on the geometry errors, so we construct bounds using the error equation, (55). For convenience, we define the volume norm of a matrix, $\underline{\mathbf{M}}$, to be

$$\|\underline{\mathbf{M}}\|_{2,\infty} = \max_{\mathcal{D}} \|\underline{\mathbf{M}}\|_2, \quad (61)$$

where $\|\underline{\mathbf{M}}\|_2 = \max_{\mathbf{w} \neq 0} \frac{\mathbf{w}^T \underline{\mathbf{M}} \mathbf{w}}{\mathbf{w}^T \mathbf{w}}$ is the matrix 2-norm. Then

$$V1 \leq \frac{1}{2} \left\| \left\| \frac{\vec{\underline{\mathbf{E}}} \cdot \nabla_{\xi} \varepsilon}{J} \right\| \right\|_{2,\infty} \|\mathbf{e}\|_J^2 \equiv c_1 \|\mathbf{e}\|_J^2, \quad V2 \leq \frac{1}{2} \left\| \left\| \frac{\vec{\underline{\mathbf{A}}} \cdot \nabla_{\xi} \varepsilon}{J} \right\| \right\|_{2,\infty} \|\mathbf{e}\|_J^2 \equiv c_2 \|\mathbf{e}\|_J^2, \quad (62)$$

where we have used the fact that the matrices are symmetric. Next, using the Cauchy-Schwarz inequality and the fact that $\vec{\underline{\mathbf{E}}}$ is divergence-free,

$$V3 \leq \left\| \left\| \frac{(1 + \varepsilon) \vec{\underline{\mathbf{E}}} \cdot \nabla_{\xi} \mathbf{q}}{J^2} \right\| \right\|_J \|\mathbf{e}\|_J \equiv c_3 \|\mathbf{e}\|_J, \quad V4 \leq \left\| \left\| \frac{\varepsilon \vec{\underline{\mathbf{A}}} \cdot \nabla_{\xi} \mathbf{q}}{J^2} \right\| \right\|_J \|\mathbf{e}\|_J \equiv c_4 \|\mathbf{e}\|_J. \quad (63)$$

The coefficients c_3 and c_4 depend on the correct solution and will serve as source terms for the error.

When we gather the terms in (56) and divide by the norm of the error,

$$\frac{d}{dt} \|\mathbf{e}\|_J + (\eta(t) - \gamma \mathcal{B}_{max} - c_1 - c_2) \|\mathbf{e}\|_J \leq c_3 + c_4, \quad (64)$$

where

$$\eta(t) = \frac{D}{\|\mathbf{e}\|_J^2}, \quad \mathcal{B} = \frac{BG}{\|\mathbf{e}\|_J^2}, \quad (65)$$

and \mathcal{B}_{max} is the maximum over the time interval. The difference $\eta(t) - \gamma \mathcal{B}_{max}$ represents the balance between the advection of error out of the domain and the error being introduced into the domain. If negative, error is injected faster than it can be removed through boundary dissipation. The remaining term, $-c_1 - c_2$, depends on ε , the error in the Jacobian. Note that $\|\mathbf{e}\|_J = 0$ only if the numerators in $\eta(t)$ and \mathcal{B} are also zero, since the norm includes the boundary values under the smoothness assumptions.

When $\eta(t) > 0$, Nordström [21] argues that $\eta(t)$ is a monotonically growing function over any finite time interval and that the mean value, $\bar{\eta}$, is bounded from below by a positive constant, that is, $\bar{\eta} \geq c_0 > 0$.

Therefore we can use an integrating factor to get the desired bound. Assuming that the correct solution, \mathbf{q} , is bounded in time so that c_3, c_4 are constant independent of time, and defining $\alpha = (c_0 - \gamma\mathcal{B}_{max} - c_1 - c_2)$,

$$\|\mathbf{e}(t)\|_J \leq e^{-\alpha t} \|\mathbf{e}(0)\|_J + (c_3 + c_4) \frac{1 - e^{-\alpha t}}{\alpha}. \quad (66)$$

Asymptotically, for large time,

$$\|\mathbf{e}(t)\|_J \leq \frac{1}{\alpha}(c_3 + c_4), \quad (67)$$

when $\alpha \geq 0$, i.e., there is sufficient outflow dissipation relative to the other errors. Eq. (67) gives the long-term error bound in terms of the geometry errors.

Remark 6. *Thm 1 already tells us that the error is bounded, but not how it is related to the boundary errors.*

From (64) and (66), we make the following observations:

1. The coefficient c_1 is a secondary quantity in that it depends on the product of two (small) error quantities; c_2 is a primary quantity. Both depend on the ratio of the Jacobians through $\nabla_\xi \varepsilon = \nabla_\xi(J/J_e)$. These terms contribute to growth in the error as a function of time.
2. It is preferred that the exact boundary locations are available at which to evaluate boundary data, i.e. $\gamma = 0$ so $\gamma\mathcal{B}_{max} = 0$. Nevertheless, \mathcal{B} varies as $|\Delta\vec{X}|^2$, and so is only a secondary quantity.
3. Even if the boundary data is specified using the exact mapping, $\gamma = 0$, errors represented by c_3 and c_4 depend on the solution, the error in the Jacobian, ε , and the volume weighted contravariant vectors (through $\vec{\mathbb{E}}$), and contribute to the persistence of the error in time.
4. The dissipation due to outgoing waves (D) that comes from using characteristic boundary conditions is necessary to keep the error bounded for long times, as it counteracts the growth due to c_1, c_2 and \mathcal{B} , which can be kept small by keeping the erroneous domain sufficiently close to the correct one.
5. As $\Omega_e \rightarrow \Omega$, $\varepsilon = J/J_e - 1 \rightarrow 0$, $\Delta J\vec{a}^i = J\vec{a}_i^* - J\vec{a}^i \rightarrow 0$ so $c_1, \dots, c_4 \rightarrow 0$. For smooth domains, $\nabla_\xi \varepsilon \rightarrow 0$ as $\Omega_e \rightarrow \Omega$, so $\|\mathbf{e}(t)\|_J \rightarrow 0$. In other words, the error converges to zero as the erroneous domain approaches the correct one.

5.1. Error Bounds for a Two Dimensional Domain with One Curved Boundary

For insight into the direct relationships between the solution error and boundary curve errors, we consider the special case of a simple geometry with one curved boundary, as seen in Fig. 2. A single boundary condition will be applied along the bottom boundary, either specified characteristic data or perfect reflection, (23).

We construct the two-dimensional mapping $\vec{X}(\vec{\xi}) = X(\xi, \eta)\hat{x} + Y(\xi, \eta)\hat{y} + 0\hat{z}$ as a transfinite interpolation [22] of the boundaries. For the simple geometry of Fig. 2, the correct transfinite mapping is

$$\vec{X}(\xi, \eta) = \vec{\Gamma}_1(\xi)(1 - \eta) + \eta\vec{\Gamma}_3(\xi) \quad (68)$$

whereas the erroneous one is

$$\vec{X}^e(\xi, \eta) = \vec{\Gamma}_1^e(\xi)(1 - \eta) + \eta\vec{\Gamma}_3(\xi), \quad (69)$$

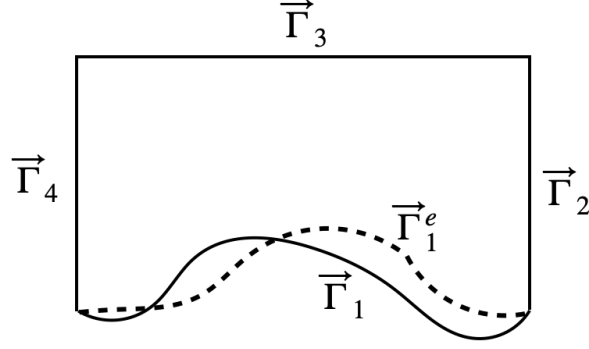


Figure 2: Correct domain (solid lines) and Erroneous domain (dashed line) boundary curves in two space dimensions used to isolate the boundary errors to one boundary

so that along the lower boundary,

$$\Delta \vec{X}(\xi, 0) = \vec{\Gamma}_1^e - \vec{\Gamma}_1 \equiv \Delta \vec{\Gamma} \quad (70)$$

is the position/location error at that boundary. The quantity $\Delta \vec{\Gamma}$ is therefore the error that appears in the boundary terms, (48), for this example. Everywhere else, its influence throughout the domain is

$$\Delta \vec{X}(\xi, \eta) = (1 - \eta) \left(\vec{\Gamma}_1^e(\xi) - \vec{\Gamma}_1(\xi) \right) = (1 - \eta) \Delta \vec{\Gamma}. \quad (71)$$

Therefore, $\Delta \vec{X}(\xi, \eta)$ is linear in $\Delta \vec{\Gamma}$, and so is the position error for any point in the reference domain.

To get the derivatives of the mapping, and from there the errors in the metric terms and Jacobians, we write the erroneous mapping as the correct mapping plus the error

$$\vec{X}^e = \vec{X} + \Delta \vec{X}. \quad (72)$$

The derivatives of the erroneous mapping

$$\begin{aligned} \vec{X}_\xi^e &= \vec{X}_\xi + \Delta \vec{X}_\xi = \vec{X}_\xi + (\vec{\Gamma}_1^{\prime, e} - \vec{\Gamma}_1') (1 - \eta) = \vec{X}_\xi + (1 - \eta) \Delta \vec{\Gamma}' \\ \vec{X}_\eta^e &= \vec{X}_\eta + \Delta \vec{X}_\eta = \vec{X}_\eta - \Delta \vec{\Gamma} \end{aligned} \quad (73)$$

are also written in terms of the correct ones.

In two space dimensions the metric terms are

$$\begin{aligned} J \vec{a}^1 &= \vec{a}_2 \times \hat{z} = \vec{X}_\eta \times \hat{z} \\ J \vec{a}^2 &= \hat{z} \times \vec{a}_1 = \hat{z} \times \vec{X}_\xi \end{aligned} \quad (74)$$

and the Jacobian is

$$J = \hat{z} \cdot (\vec{a}_1 \times \vec{a}_2) = \hat{z} \cdot (\vec{X}_\xi \times \vec{X}_\eta). \quad (75)$$

So on the erroneous domain,

$$\begin{aligned} J \vec{a}_e^1 &= J \vec{a}^1 - \Delta \vec{\Gamma} \times \hat{z} \\ J \vec{a}_e^2 &= J \vec{a}^2 + (1 - \eta) \hat{z} \times \Delta \vec{\Gamma}'. \end{aligned} \quad (76)$$

So we see that the metric term errors depend on $\Delta \vec{\Gamma}$ and its derivative $\Delta \vec{\Gamma}'$,

$$\begin{aligned} \Delta J \vec{a}^1 &= \hat{z} \times \Delta \vec{\Gamma} \\ \Delta J \vec{a}^2 &= (1 - \eta) \hat{z} \times \Delta \vec{\Gamma}'. \end{aligned} \quad (77)$$

The vector $J\vec{a}_e^2(\xi, 0)$ is in the inward normal direction to the erroneous boundary, with the correct outward unit normal being

$$\hat{n} = \frac{\vec{n}}{|\vec{n}|} = -\frac{J\vec{a}^2}{|J\vec{a}^2|}. \quad (78)$$

The error matrices (37) are

$$\tilde{\underline{E}}^i = \Delta J\vec{a}^i \cdot \vec{\underline{A}}, \quad (79)$$

or, explicitly

$$\begin{aligned} \tilde{\underline{E}}^1 &= \vec{\underline{A}} \cdot \left(\hat{z} \times \Delta\vec{\Gamma} \right) = \hat{z} \cdot \left(\Delta\vec{\Gamma} \times \vec{\underline{A}} \right) \\ \tilde{\underline{E}}^2 &= (1 - \eta)\vec{\underline{A}} \cdot \left(\hat{z} \times \Delta\vec{\Gamma}' \right) = (1 - \eta)\hat{z} \cdot \left(\Delta\vec{\Gamma}' \times \vec{\underline{A}} \right). \end{aligned} \quad (80)$$

So the error matrices are also linear in $\Delta\vec{\Gamma}$ and $\Delta\vec{\Gamma}'$. The first, $\tilde{\underline{E}}^1$, is the error due to location of the boundary. The second, $\tilde{\underline{E}}^2$, is the error due to the error in the tangent to, or derivative, along the boundary, and also represents the error in the normal there.

The error in the erroneous Jacobian is bilinear in $\Delta\vec{\Gamma}$ and $\Delta\vec{\Gamma}'$, for

$$\begin{aligned} J_e &= \hat{z} \cdot \left(\left(\vec{X}_\xi + (1 - \eta)\Delta\vec{\Gamma}' \right) \times \left(\vec{X}_\eta - \Delta\vec{\Gamma} \right) \right) \\ &= \hat{z} \cdot \left\{ \left(\vec{X}_\xi \times \vec{X}_\eta \right) - \left(\vec{X}_\xi \times \Delta\vec{\Gamma} \right) + (1 - \eta) \left(\Delta\vec{\Gamma}' \times \vec{X}_\eta \right) - (1 - \eta) \left(\Delta\vec{\Gamma}' \times \Delta\vec{\Gamma} \right) \right\} \\ &= J + \hat{z} \cdot \left\{ \left(\Delta\vec{\Gamma} \times \vec{X}_\xi \right) + (1 - \eta) \left(\Delta\vec{\Gamma}' \times \vec{X}_\eta - \Delta\vec{\Gamma}' \times \Delta\vec{\Gamma} \right) \right\} \\ &\equiv J + \epsilon. \end{aligned} \quad (81)$$

In terms of the Jacobian error, the ratio of the Jacobians is

$$\rho = \frac{J}{J_e} = \frac{J}{J + \epsilon}, \quad (82)$$

and so

$$\varepsilon = \rho - 1 = -\frac{\epsilon}{J + \epsilon}. \quad (83)$$

We see that ε is nonlinear in the location and derivative errors. However, ϵ will presumably be small, so we will write

$$\rho = \frac{1}{1 + \epsilon/J} = 1 - \frac{\epsilon}{J} + O(\epsilon^2). \quad (84)$$

To lowest order, $\varepsilon \approx -\epsilon/J$ and is bilinear in $\Delta\vec{\Gamma}$ and $\Delta\vec{\Gamma}'$.

Let us gather the geometric errors and use three unit vectors defined as

$$\hat{\alpha} = \frac{\Delta\vec{\Gamma}}{|\Delta\vec{\Gamma}|}, \quad \hat{\beta} = \frac{\Delta\vec{\Gamma}'}{|\Delta\vec{\Gamma}'|}, \quad \hat{\gamma} = \frac{\Delta\vec{\Gamma}''}{|\Delta\vec{\Gamma}''|} \quad (85)$$

to write them as

$$\begin{aligned}
\Delta \vec{X} &= (1 - \eta) \left| \Delta \vec{\Gamma} \right| \hat{\alpha} \\
\tilde{\mathbf{E}}^1 &= \left| \Delta \vec{\Gamma} \right| \hat{z} \cdot \left(\hat{\alpha} \times \vec{\mathbf{A}} \right) \equiv \left| \Delta \vec{\Gamma} \right| \hat{\mathbf{A}}_1, \\
\tilde{\mathbf{E}}^2 &= (1 - \eta) \left| \Delta \vec{\Gamma}' \right| \hat{z} \cdot \left(\hat{\beta} \times \vec{\mathbf{A}} \right) \equiv (1 - \eta) \left| \Delta \vec{\Gamma}' \right| \hat{\mathbf{A}}_2 \\
\epsilon &= \hat{z} \cdot \left\{ \left(\hat{\alpha} \times \vec{X}_\xi \right) \left| \Delta \vec{\Gamma} \right| + (1 - \eta) \left(\hat{\beta} \times \vec{X}_\eta \right) \left| \Delta \vec{\Gamma}' \right| - (1 - \eta) \left| \Delta \vec{\Gamma}' \right| \left| \Delta \vec{\Gamma} \right| \left(\hat{\alpha} \times \hat{\beta} \right) \right\} \\
&\equiv r_1 \left| \Delta \vec{\Gamma} \right| + (1 - \eta) r_2 \left| \Delta \vec{\Gamma}' \right| + (1 - \eta) r_3 \left| \Delta \vec{\Gamma}' \right| \left| \Delta \vec{\Gamma} \right| \\
\rho &= \frac{J}{J + \epsilon} = 1 - \frac{\epsilon}{J} + O(\epsilon^2) \\
\varepsilon &= -\frac{\epsilon}{J + \epsilon} = -\frac{\epsilon}{J} + O(\epsilon^2).
\end{aligned} \tag{86}$$

Note that the functions used in ϵ ,

$$r_1 = \hat{z} \cdot \left(\hat{\alpha} \times \vec{X}_\xi \right), \quad r_2 = \hat{z} \cdot \left(\hat{\beta} \times \vec{X}_\eta \right), \quad r_3 = -\hat{z} \cdot \left(\hat{\alpha} \times \hat{\beta} \right), \tag{87}$$

are bounded by the size of the correct mapping derivatives, $\vec{X}_\xi, \vec{X}_\eta$. The matrices

$$\hat{\mathbf{A}}_1 = \hat{z} \cdot \left(\hat{\alpha} \times \vec{\mathbf{A}} \right), \quad \hat{\mathbf{A}}_2 = \hat{z} \cdot \left(\hat{\beta} \times \vec{\mathbf{A}} \right) \tag{88}$$

are bounded by $\max_{|\hat{w}| \leq 1} \left\| \hat{\mathbf{A}}_i \cdot \hat{w} \right\|_2$, the norm being the spectral radius. Therefore, all error quantities in (86) are bounded, and to lowest order are proportional to $\left| \Delta \vec{\Gamma} \right|$ and $\left| \Delta \vec{\Gamma}' \right|$.

Thus, we see that as $\Delta \vec{\Gamma} \rightarrow 0$ and $\Delta \vec{\Gamma}' \rightarrow 0$, the geometry errors $\epsilon \rightarrow 0$ and $\tilde{\mathbf{E}} \rightarrow 0$ and so by (67), $\|e\|_J \rightarrow 0$.

From the geometric errors, we find how the global error depends on errors in the boundary curve for the specified data boundary condition. The perfectly reflecting boundary condition does not introduce additional error (its contribution is zero) but merely reflects it, albeit in the wrong direction, so we need only consider the specified boundary value error. In the process, let us rewrite (56) as

$$\begin{aligned}
\|e\|_J \frac{d}{dt} \|e\|_J + \frac{1}{2} \int_0^1 \mathbf{e}^T \underline{\mathbf{A}}^+ \mathbf{e} \Big|_{\eta=0} d\xi &= -D1 - D2 + \gamma DG + V1 + V2 + V3 + V4 \\
&\equiv \mathcal{R},
\end{aligned} \tag{89}$$

where $D1, D2, DG$ are the dissipation and boundary errors defined in (B.13), (B.15), (B.16), and we have used the fact that the boundary errors are nonzero only along the $\vec{\Gamma}_1$ boundary.

The functional, \mathcal{R} , contains all the error terms controllable by the accuracy of $\vec{\Gamma}_1$. In Appendix B, we show that

$$\begin{aligned}
|\mathcal{R}(\Delta \vec{\Gamma}, \Delta \vec{\Gamma}', \Delta \vec{\Gamma}'')| &\leq \left| \Delta \vec{\Gamma} \right|_{max} \left\{ \frac{1}{2} \left\| \frac{\mathbf{M}_1}{J} \right\|_{2,\infty} \|e\|_J + \left\| \frac{\hat{\mathbf{A}}_1 \mathbf{q}_\xi}{J^2} \right\|_J + \left\| \frac{r_1 \left(\vec{\mathbf{A}} \cdot \nabla_\xi \mathbf{q} \right)}{J^3} \right\|_J \right\} \|e\|_J \\
&+ \left| \Delta \vec{\Gamma}' \right|_{max} \left\{ \frac{1}{2} \left\| \frac{\mathbf{M}_2}{J} \right\|_{2,\infty} \|e\|_J + \left\| \frac{(1 - \eta) \hat{\mathbf{A}}_2 \mathbf{q}_\eta}{J^2} \right\|_J + \left\| \frac{(1 - \eta) r_2 \left(\vec{\mathbf{A}} \cdot \nabla_\xi \mathbf{q} \right)}{J^3} \right\|_J \right\} \|e\|_J \\
&+ \left| \Delta \vec{\Gamma}'' \right|_{max} \left\{ \frac{1}{2} \left\| \frac{\mathbf{M}_3}{J} \right\|_{2,\infty} \|e\|_J \right\} \|e\|_J + HOTs,
\end{aligned} \tag{90}$$

where the matrices $\underline{M}_1, \underline{M}_2, \underline{M}_3$ are defined in (B.7). The first term in each brace in (90) contributes to the exponential behavior of the error in time through the coefficient α in (66). The remaining terms depend on the correct solution and act as source terms, affecting the size of the long term error through c_3 and c_4 . The \mathcal{B}_{max} term in (64) is second and higher order.

The long term error depends on the size of c_3 and c_4 , see (67). Using the definitions for c_3, c_4 in (63), and the bounds from (B.11) and (B.12) in Appendix B,

$$c_3 + c_4 = \left| \Delta \vec{\Gamma} \right|_{max} \left\{ \left\| \frac{\hat{\mathbf{A}}_1 \mathbf{q}_\xi}{J^2} \right\|_J + \left\| \frac{r_1 \left(\vec{\mathbf{A}} \cdot \nabla_\xi \mathbf{q} \right)}{J^3} \right\|_J \right\} \\ + \left| \Delta \vec{\Gamma}' \right|_{max} \left\{ \left\| \frac{(1-\eta) \hat{\mathbf{A}}_2 \mathbf{q}_\eta}{J^2} \right\|_J + \left\| \frac{(1-\eta) r_2 \left(\vec{\mathbf{A}} \cdot \nabla_\xi \mathbf{q} \right)}{J^3} \right\|_J \right\} + HOT_s \quad (91)$$

From (91) and (67), we conclude that for long times to the lowest order, the global error is proportional to the magnitude of the location error $\Delta \vec{\Gamma}$ and to the magnitude of the derivative error $\Delta \vec{\Gamma}'$. The coefficient of $\left| \Delta \vec{\Gamma}' \right|_{max}$ depends on $(1-\eta)$, which vanishes at the upper boundary. All things being equal, that factor makes those coefficients smaller than the coefficients of $\left| \Delta \vec{\Gamma} \right|_{max}$ for the simple geometry in Fig. 2. Finally, then, from (67), we see that the error converges linearly with $\Delta \vec{\Gamma}$ and $\Delta \vec{\Gamma}'$ as $\Omega_e \rightarrow \Omega$.

Remark 7. *The dependence, $1-\eta$, in the influence of the derivative error on the solution error is a result of the transfinite interpolation with linear blending for the mapping, and reflects the fact that the bottom boundary does not affect top one.*

6. Examples

We present two examples to show the linear variation of the error with respect to boundary location and derivative errors. The first, in one space dimension, can be studied from the analytic solution, but contains only boundary location error. The second, in two space dimensions, has the single boundary curve error of Fig. 2.

6.1. The Scalar Advection Equation in one Space Dimension

The first example solves the IBVP for the constant coefficient scalar advection equation

$$q_t + a q_x = 0, \quad x \in \Omega = [0, 1], a > 0 \\ q(0, t) = -\sin(2\pi a t) \\ q(x, 0) = \sin(2\pi x). \quad (92)$$

In this case, $\Omega = \mathcal{D}$, $J = 1$, and $\xi = x$. The correct solution is $q(\xi, t) = \sin(2\pi(\xi - at))$.

Now let $\Omega_e = [\delta, 1]$, $\delta < 1$, be the erroneous domain. Transforming to the unit reference domain,

$$X_e = \delta + \xi(1 - \delta), \quad J_e = \frac{\partial x}{\partial \xi} = 1 - \delta, \quad (93)$$

so that from (70), $\Delta X(\xi) = (1 - \xi)\delta$, and from (73), $J \hat{a}^{-1} = 1 \hat{x}$. Then the erroneous domain problem becomes

$$v_t + \frac{a}{(1 - \delta)} v_\xi = 0 \\ v(0, t) = g_\gamma(\xi, t) \\ v(x, 0) = \sin(2\pi(\delta + \xi(1 - \delta))) \quad (94)$$

We consider two choices for the boundary value $g_\gamma(\xi, t)$, namely

$$g_\gamma = \sin(2\pi(\gamma\delta - at)) \quad (95)$$

with $\gamma = 0$ and $\gamma = 1$. As used above in (54), g_0 is exact at the left boundary, and no error is introduced there. For g_1 , the boundary value is evaluated at the erroneous location, and hence introduces error there. The analytic solution for the erroneous domain is then

$$v(\xi, t) = \begin{cases} \sin\left(2\pi\left(\delta + \xi(1-\delta) - \frac{a}{1-\delta}t\right)\right) & \xi - \frac{a}{1-\delta}t > 0 \\ -\sin\left(2\pi a\left(t - \frac{\gamma\delta + \xi(1-\delta)}{a}\right)\right) & \xi - \frac{a}{1-\delta}t \leq 0 \end{cases}. \quad (96)$$

In Sec. 5 we showed what quantities affect the error and its bounds. For the one dimensional scalar problem here,

$$\varepsilon = \frac{1}{1-\delta} - 1 = \frac{\delta}{1-\delta} = \delta\rho \quad (97)$$

so that $\nabla_\xi \varepsilon = 0$. Next, $\vec{\mathbf{E}} = 0$ since $J\vec{\mathbf{a}}^{-1} = J\vec{\mathbf{a}}_e^{-1} = 1\hat{x}$. Then $c_1 = c_2 = 0$ and $c_3 = 0$ in (64). But $c_4 = 2\pi|\delta/(1-\delta)|$, since the correct solution is sinusoidal. When $\gamma = 0$, $e_g = 0$, and the inflow boundary term, \mathcal{B} , vanishes. Then with the dissipation, D , included at the right boundary,

$$\frac{d}{dt} \|e(t)\|_J + \left[\frac{ae^2(1, t)}{\|e(t)\|_J^2} \right] \|e(t)\|_J \leq \frac{4\pi|\delta|}{1-\delta} = 4\pi|\delta|\rho, \quad (98)$$

which, since ρ is a constant, we write as

$$\frac{d}{dt} \|e(t)\|_J + \rho\eta(t) \|e(t)\|_J \leq 4\pi|\delta|\rho. \quad (99)$$

As before, the mean value of $\eta(t)$ over any finite time interval, $\bar{\eta}$, is bounded from below by a positive constant, i.e., $\bar{\eta} \geq c_0 > 0$ and therefore we can use an integrating factor to the bound

$$\|e(t)\|_J \leq e^{-\rho c_0 t} \|e(0)\|_J + \frac{1 - e^{-\rho c_0 t}}{\rho c_0} 4\pi|\delta|\rho = e^{-\rho c_0 t} \|e(0)\|_J + \frac{1 - e^{-\rho c_0 t}}{c_0} 4\pi|\delta|. \quad (100)$$

As seen in Sec. 5 for the general case, (100) says that the error is bounded in time, for large time it approaches $4\pi|\delta|/c_0$, and it varies linearly with the boundary location error, δ . We also argued in Sec. 5 that the boundary value evaluation error introduced when applying the boundary condition at the wrong point in space ($\gamma = 1$) should not change this result significantly, since that term is a secondary quantity. In other words, the dominant error should be due to the volume errors.

When we measure the norm of the error, it is bounded, as predicted, for both $\gamma = 0$ and $\gamma = 1$. Fig. 3 shows the time history of the norm of the error for two values of δ and for both values of γ . As expected, the error is larger for the larger boundary location error, 0.283 for $\delta = 0.1$ and 0.143 for $\delta = 0.05$. The ratio of the two, 1.98, confirms the linear variation with δ . Further confirmation of the linear behavior of the maximum error for small $|\delta|$ is shown in Fig. 4, which plots the peak value of the error for large time seen in Fig. 3 as a function of δ for both positive and negative values of δ . Finally, Figs. 3 and 4 also confirm that the boundary value error, \mathcal{B} , does not significantly impact the maximum of the L^2 norm of the error for long times, since the maximum errors are indistinguishable between $\gamma = 0$ and $\gamma = 1$.

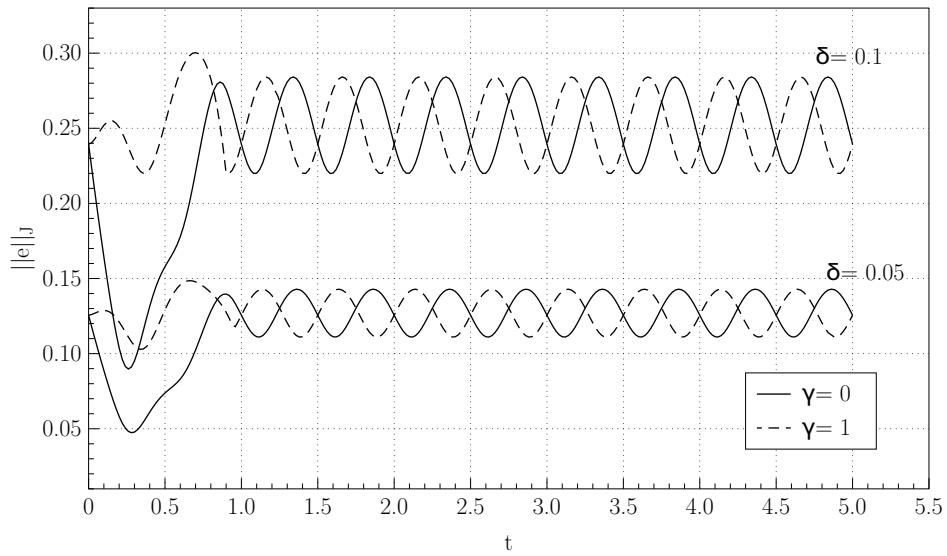


Figure 3: Time history of the error for two values of the left boundary location error, δ , and for two values of γ for the one dimensional scalar problem, (92)

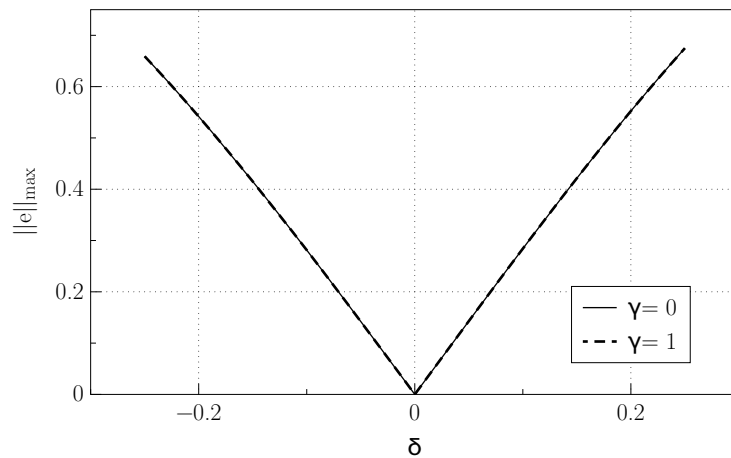


Figure 4: Variation of the maximum errors as a function of δ for the large time solution of the one dimensional scalar problem, (92)

6.2. The Scalar Advection Equation in Two Space Dimensions

We illustrate the errors in two space dimensions for the correct domain $\Omega = [0, 1]^2$ and erroneous domains with

$$\vec{X}(\xi, \eta) = \vec{\Gamma}_1(\xi)(1 - \eta) + \eta[\xi\hat{x} + 1\hat{y}]. \quad (101)$$

We choose four erroneous domains, two with a linear lower boundary and two with a quadratic one, see Fig. 5. For two domains, one or two points match the endpoints of the correct bottom curve. The other two are the minimax polynomial approximations of degree one or two. The bottom curves for the four cases are

$$\begin{aligned} \Omega_e^{(1)} : \Gamma_1^e(\xi) &= \xi\hat{x} - \delta\xi\hat{y} \\ \Omega_e^{(2)} : \Gamma_1^e(\xi) &= \xi\hat{x} - \delta\left(\xi - \frac{1}{2}\right)\hat{y} \\ \Omega_e^{(3)} : \Gamma_1^e(\xi) &= \xi\hat{x} + 4\delta\xi(\xi - 1)\hat{y} \\ \Omega_e^{(4)} : \Gamma_1^e(\xi) &= \xi\hat{x} + \left(4\delta\xi(\xi - 1) + \frac{1}{2}\delta\right)\hat{y}. \end{aligned} \quad (102)$$

The parameter δ controls the deviation of the erroneous domain from the correct one, and also the error in the derivative.

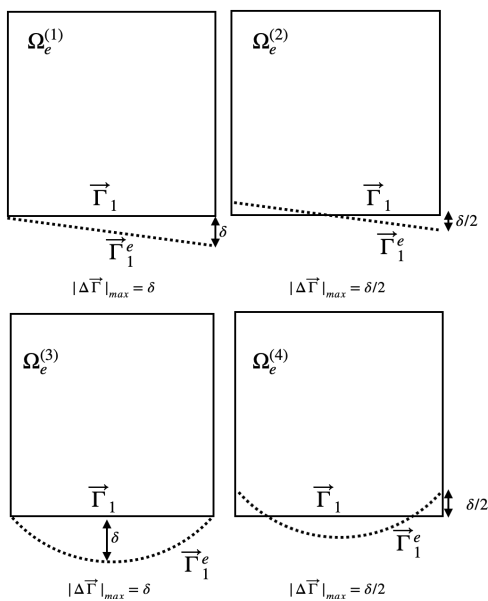


Figure 5: Correct and erroneous domains in two space dimensions with linear and quadratic perturbations. On the left, the approximate curve matches at least one end point. On the right is the minimax approximation

The IBVP solved is

$$\begin{aligned} q_t + \vec{a} \cdot \nabla_x q &= 0, \quad \vec{a} = a_1\hat{x} + a_2\hat{y} > 0, \quad x \in \Omega, t > 0 \\ q(0, y, t) &= f(a_2y - |a|^2t) \\ q(x, y, t) &= f(\vec{a} \cdot \vec{\Gamma}_1 - |a|^2t), \quad \vec{x} \in \vec{\Gamma}_1 \\ q(x, y, 0) &= f(a_1x + a_2y), \end{aligned} \quad (103)$$

which has the analytic solution

$$q(x, y, t) = f(\vec{a} \cdot \vec{x} - |a|^2t). \quad (104)$$

For the examples here we choose $f(\phi) = \sin(\omega\pi\phi)$ with $\omega = 4$, and $\vec{a} = (\sqrt{3}/2, 1/2)$ so that $|a| = 1$.

Since this problem becomes variable coefficient in the erroneous domain, we compute its solution numerically with a single domain discontinuous Galerkin Spectral Element approximation, [23, Sec. 7.4]. We compute the solutions so that the approximation errors are small compared to the erroneous domain errors. We choose a polynomial approximation order of $N = 18$ and time step $\Delta t = 1 \times 10^{-4}$ so that the approximation errors were 3.2×10^{-8} for the correct domain and less than 6×10^{-6} for any of the erroneous domains at the chosen final time, $t = 1.5$. Finally, since the boundaries are (at most) polynomials of degree two, the boundary mappings and metric terms are represented exactly by the approximations.

Eqs. (67) and (91) imply that the domain error should vary linearly with $|\Delta\vec{\Gamma}|_{max}$ for small δ . For the linear domain, $\Omega_e^{(1)}$ (see Fig. 5),

$$|\Delta\vec{\Gamma}|_{max} = |\delta|, \quad |\Delta\vec{\Gamma}'|_{max} = \frac{1}{2}|\delta|, \quad |\Delta\vec{\Gamma}''|_{max} = 0 \quad (105)$$

and for the quadratic,

$$|\Delta\vec{\Gamma}|_{max} = |\delta|, \quad |\Delta\vec{\Gamma}'|_{max} = |\delta|, \quad |\Delta\vec{\Gamma}''|_{max} = 2|\delta|. \quad (106)$$

For the minimax approximations the $|\Delta\vec{\Gamma}|_{max}$ quantities are halved, but the others remain the same. Thus, as long as the coefficients for the perturbation quantities in (B.17) remain constant, the errors should be linear in δ . Furthermore, for each of these erroneous domains, $r_2 = 0$ (see (87)), making the $|\Delta\vec{\Gamma}|_{max}$ error term dominant in (90), so the error for the minimax approximations should be roughly half of the others.

In Fig. 6 we plot the error as a function of δ for the linear erroneous domains and see that it grows linearly, as predicted. The ratio of the slopes is 2.04, which indicates that the error is dominated by the $|\Delta\vec{\Gamma}|_{max}$ term. We can compute bounds for the coefficients in (91), and find that $R \leq 25.4|\Delta\vec{\Gamma}|_{max} + 4.52|\Delta\vec{\Gamma}'|_{max} + HOTs$ for $\Omega_e^{(1)}$. In Fig. 6 we also plot the error as a function of δ for the quadratic

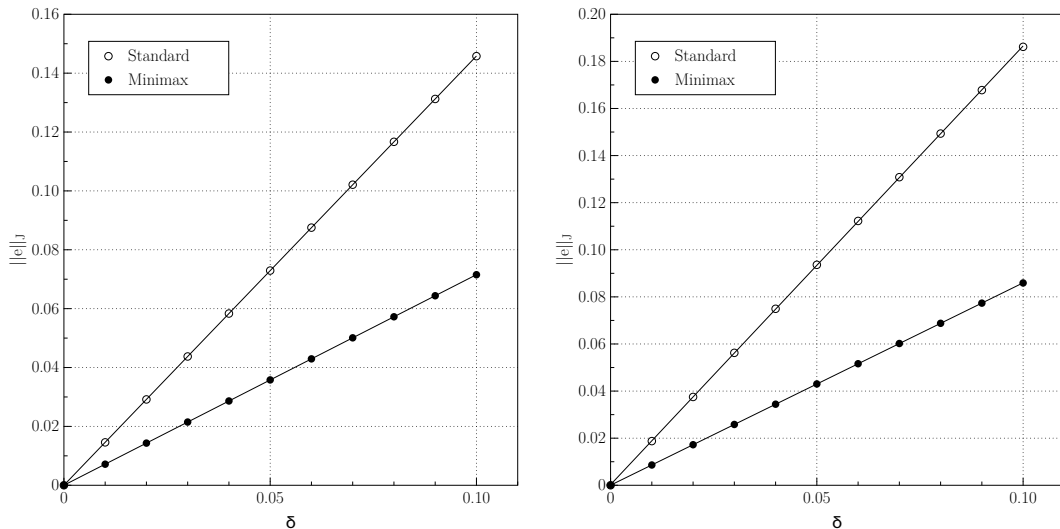


Figure 6: Growth of the erroneous domain error as a function of perturbation parameter δ for the standard ($\Omega_e^{(1)}$) and minimax ($\Omega_e^{(2)}$) linear erroneous domains (left) and for the ($\Omega_e^{(3)}$) and minimax ($\Omega_e^{(4)}$) quadratic erroneous domains (right). Circles are the measured values and the lines are the linear least squares approximations through those points

erroneous domains and see that it, too, grows linearly, as expected. The ratio of the slopes is 2.18,

which also indicates that the error is dominated by the $|\Delta\vec{\Gamma}|_{max}$ term. When we compute bounds for the coefficients in (91), we find that $R \leq 27.2|\Delta\Gamma|_{max} + 3.9|\Delta\Gamma'|_{max} + HOTs$ for $\Omega_e^{(3)}$.

We can isolate the effects of the errors in the location and the derivative in (91) by using the correct values for one and the erroneous values for the other when constructing the geometry and metric terms. For instance, ‘‘Correct Location/Erroneous Derivative’’ corresponds to $\Delta\vec{\Gamma} = 0$ and $\Delta\vec{\Gamma}' = -\delta$ for $\Omega_e^{(1)}$. In each case, the error should vary linearly in the parameter δ . Fig. 7 shows that the error does vary linearly for $\Omega_e^{(1)}$ and $\Omega_e^{(3)}$. Fig. 8 shows the same for the minimax approximations $\Omega_e^{(2)}$ and $\Omega_e^{(4)}$. We note that for the isolated errors, the errors in the derivative have a significant impact on the solution error, with the slopes differing by up to 42% for the examples presented.

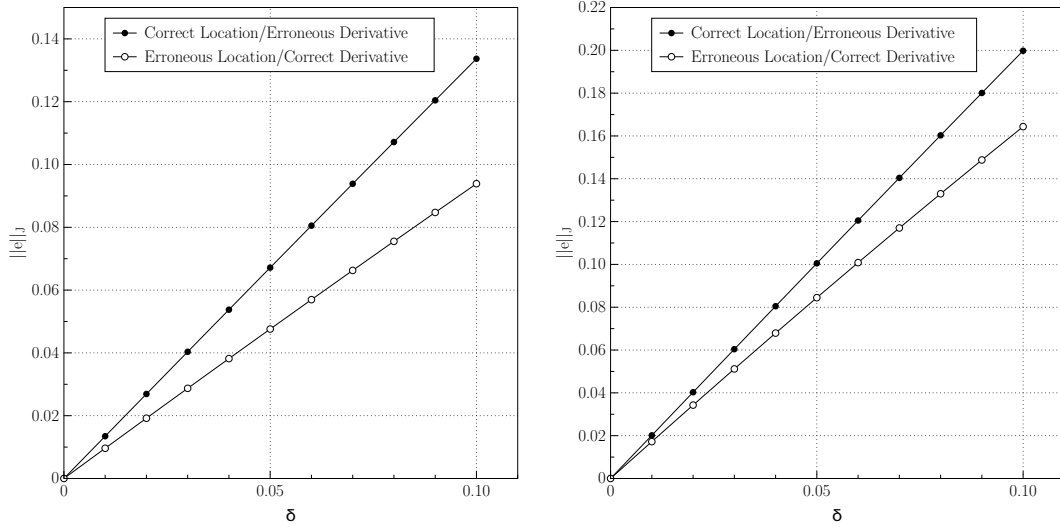


Figure 7: Isolated errors as a function of δ for $\Omega_e^{(1)}$ (left) and $\Omega_e^{(3)}$ (right)

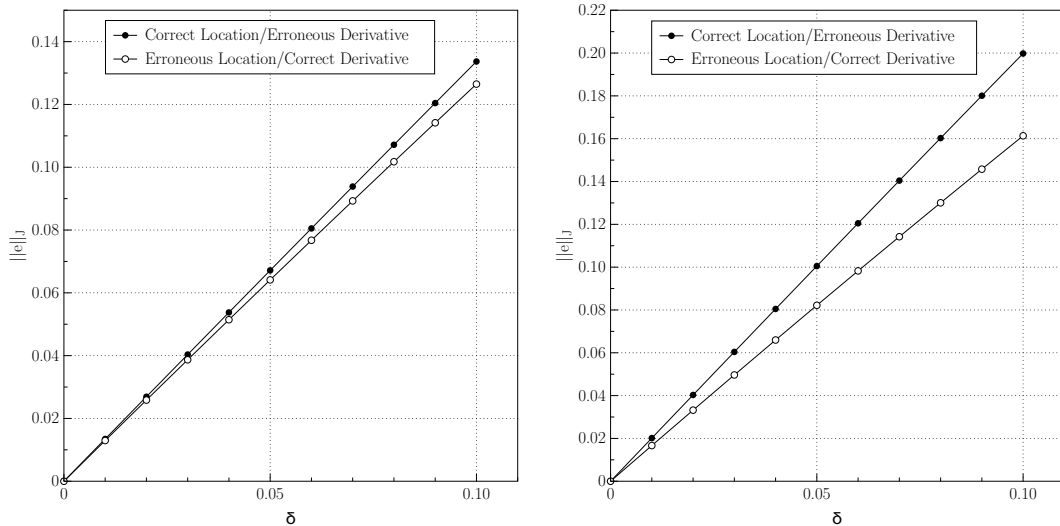


Figure 8: Isolated errors as a function of δ for the mini-max approximations, $\Omega_e^{(2)}$ (left) and $\Omega_e^{(4)}$ (right)

For the final example we choose a circular arc domain shown in Fig. 9, which has a circular domain boundary that will be approximated by quadratic polynomials. We use two parametrizations of the

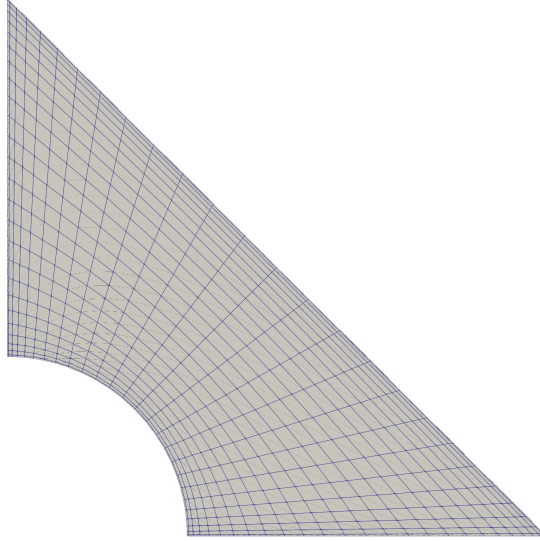


Figure 9: Correct domain with a circular boundary

circular boundary. The first is the x-parametrization,

$$\begin{aligned} x &= \xi \\ y &= \sin\left(\frac{\pi}{2}(1 - \xi)\right) \end{aligned} \tag{107}$$

with the nodes equally spaced placed at $\xi = [0, 0.5, 1]$. The second is the arc length parametrization,

$$\begin{aligned} x &= \cos\left(\frac{\pi}{2}(1 - \xi)\right) \\ y &= \sin\left(\frac{\pi}{2}(1 - \xi)\right), \end{aligned} \tag{108}$$

again, with equally spaced nodes. The differences in the curves and their derivatives are shown in Fig. 10. The errors in location and derivatives are shown in Fig. 11. Table 1 shows the maximum errors and their ratios.

Table 1: Errors for the two parametrizations for the circle

Approximation	$ \Delta\vec{\Gamma} _{max}$	$ \Delta\vec{\Gamma}' _{max}$	$\ e\ _J$
x-Parametrization	0.27	1.34	0.598
Arc Length	0.030	0.31	0.0536
Ratio:	8.9	4.33	11.1

We solve the same PDE problem as in the previous examples with $N = 26$ to get errors less than 1.1×10^{-7} for both the correct and erroneous domains. The commonly used arc length parametrization gives the better error by an order of magnitude, as seen in Table 1, which also shows the solution errors and their ratios.

7. Summary and Conclusions

Except in the simplest of geometries, the boundaries of meshes on which numerical solutions of PDEs are computed are only approximations to the true boundaries. The boundary approximation error is one

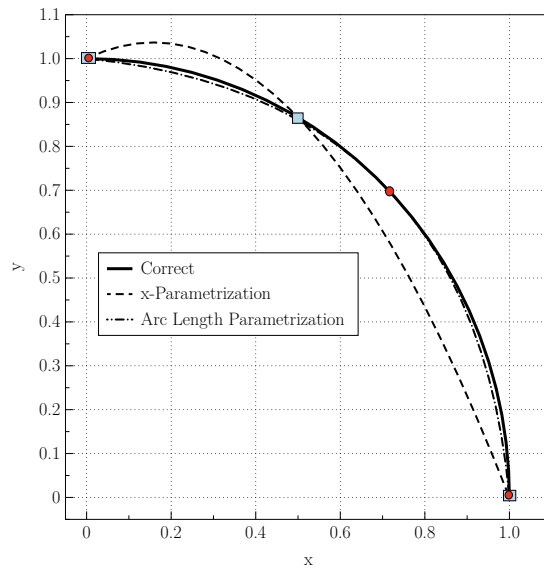


Figure 10: Quadratic approximations of the quarter circle using the x-parametrization (107) and arc length parametrization (108). Squares mark the nodes of the x-parametrization, circles the arc length parametrization

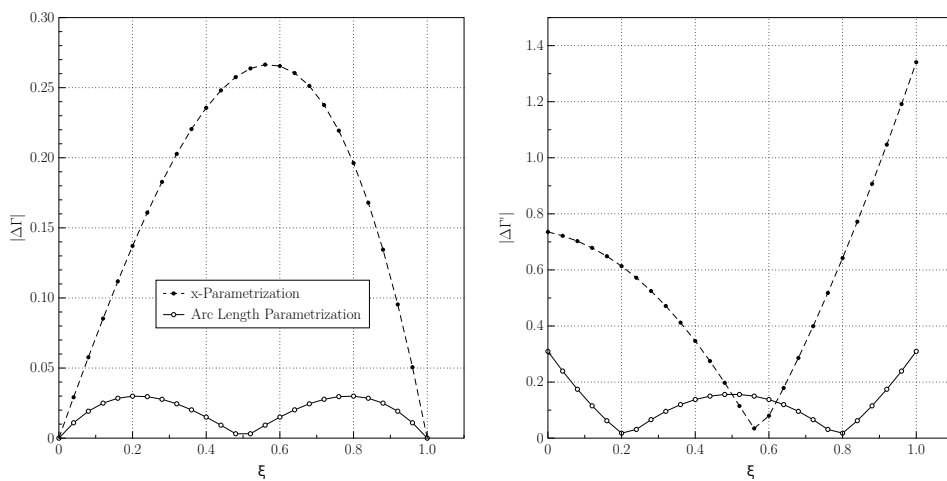


Figure 11: Errors in location (left) and derivatives (right) for the quadratic polynomial approximation of the circle

component of the total error in a numerical computation. It is one that is not controlled by the PDE solver, and is especially important for high-order solvers where the solver error could be less than the geometry error. Acknowledgment of this has led to optimization procedures at the mesh generation stage. What has been previously lacking, particularly for hyperbolic systems, is a derivation of the relationship between boundary approximation errors and solution errors.

We have derived the global, L^2 , error for linear hyperbolic systems generated by errors in the boundary geometry. We show that the error is bounded by data, and is bounded in time if the true solution is bounded in time.

The total error, (55), depends both on volume and boundary errors. The dominant volume errors depend on $\rho = J/J_e = J/(J + \epsilon)$ and $\Delta J \bar{a}^i = J \bar{a}_e^i - J \bar{a}^i$. Along the boundaries, the latter quantities correspond to the errors in the normals. To minimize the volume sources of error in (55), then, one would want to minimize the controllable quantities $\epsilon = \Delta J$ and $\Delta J \bar{a}^i$ over the reference domain. The errors introduced by the boundary conditions appear in the amount of dissipation for outgoing waves, and in the error introduced by evaluating the boundary condition at the wrong location. The boundary location error is second order in the location error, however, whereas the volume error is first order. Therefore, *it is not enough to simply evaluate the boundary conditions at the correct locations, even if those are available, to eliminate the error*. Finally, the results imply that for a numerical computation to converge at the expected rate, the boundary approximations must also converge at the same order.

We also isolated the effects of a boundary approximation by deriving the error due to a single boundary curve in two space dimensions. There, the error depends to first order on the location error, its derivative, and its second derivative. The numerical experiments here demonstrate this behavior, as do the manufactured solutions in [14]. This suggests that it is desirable to include the error in the normals, through the derivatives of the boundary, as part of an optimization procedure, e.g. as in [12],[10].

The analysis presented here is limited to linear, constant coefficient, systems. More importantly, the error as measured by the L^2 norm does not address all the important errors in the analysis of hyperbolic systems, where phase errors are also crucially important. The global L^2 error, for instance, is not affected by errors at perfectly reflecting (e.g. wall) boundaries, but the normal directions have a critical effect on reflection directions and therefore the locations of nodes and anti-nodes. Thus, there is room for further analysis of the errors due to inaccurate boundary approximation for hyperbolic problems.

Acknowledgments

This work was supported by grants from the Simons Foundation (#426393,#961988, David Kopriva). Andrew Winters was supported by Vetenskapsrådet, Sweden [award no. 2020-03642 VR]. Jan Nordström was supported by Vetenskapsrådet, Sweden [award no. 2021-05484 VR] and the University of Johannesburg Global Excellence and Stature Initiative Funding.

CRedit authorship contribution statement

David Kopriva: Concept, Derivations, Software, Visualization, Writing — original draft.

Andrew R. Winters: Concept, Methodology, Writing.

Declaration of competing interest

The authors declare that they have no known competing financial interests or personal relationships that could have appeared to influence the work reported in this paper.

Data availability

The code used to create the results herein is available upon request to the corresponding author.

Appendix A. Boundary Matrix Splittings

For any matrix $\underline{\mathbf{M}}$ that is similar to a diagonal matrix, its eigenvalue splitting can be written as

$$\underline{\mathbf{M}} = \frac{1}{2}(\underline{\mathbf{M}} + |\underline{\mathbf{M}}|) + \frac{1}{2}(\underline{\mathbf{M}} - |\underline{\mathbf{M}}|) \equiv \underline{\mathbf{M}}^+ + \underline{\mathbf{M}}^-. \quad (\text{A.1})$$

Therefore, for the boundary matrix $\underline{\mathbf{B}} = \underline{\mathbf{A}} + \underline{\mathbf{E}}$,

$$\underline{\mathbf{B}} = \underline{\mathbf{B}}^+ + \underline{\mathbf{B}}^- = \underline{\mathbf{A}}^+ + \underline{\mathbf{A}}^- + \underline{\mathbf{E}}^+ + \underline{\mathbf{E}}^-. \quad (\text{A.2})$$

Gathering terms,

$$\underline{\mathbf{B}}^+ + \underline{\mathbf{B}}^- = (\underline{\mathbf{A}}^+ + \underline{\mathbf{E}}^+) + (\underline{\mathbf{A}}^- + \underline{\mathbf{E}}^-). \quad (\text{A.3})$$

The first term on each side of (A.3) is non-negative, and the second is non-positive. The matrices do not commute, since the eigenvectors of $\underline{\mathbf{B}}$ depend on $J\vec{a}_e^i$, $\underline{\mathbf{A}}$ on $J\vec{a}_e^i$, and $\underline{\mathbf{E}}$ on $\Delta J\vec{a}_e^i$. Since they don't commute, $\underline{\mathbf{B}}^\pm \neq \underline{\mathbf{A}}^\pm + \underline{\mathbf{E}}^\pm$, but for erroneous domains that closely approximate the correct domain, $\underline{\mathbf{B}}^\pm \approx \underline{\mathbf{A}}^\pm + \underline{\mathbf{E}}^\pm$. When setting boundary conditions on the term $\mathbf{e}^T \underline{\mathbf{B}} \mathbf{e}$, two boundary term options are

$$\mathbf{e}^T \underline{\mathbf{B}}^+ \mathbf{e} + \mathbf{e}_g^T \underline{\mathbf{B}}^- \mathbf{e}_g \approx \mathbf{e}^T (\underline{\mathbf{A}}^+ + \underline{\mathbf{E}}^+) \mathbf{e} + \mathbf{e}_g^T (\underline{\mathbf{A}}^- + \underline{\mathbf{E}}^-) \mathbf{e}_g, \quad (\text{A.4})$$

where \mathbf{e}_g is the boundary error. Both will give desired bounds, but those bounds will be different depending on how well $\underline{\mathbf{B}}^\pm$ is approximated by $\underline{\mathbf{A}}^\pm$ and $\underline{\mathbf{E}}^\pm$.

Finally, we can also write the erroneous normal characteristic matrices in terms of the correct matrices plus an error matrix,

$$\underline{\mathbf{B}}^\pm = \underline{\mathbf{A}}^\pm + \underline{\mathbf{E}}^{*,\pm}, \quad (\text{A.5})$$

where, now, $\underline{\mathbf{E}}^{*,\pm} \approx \underline{\mathbf{E}}^\pm$. So a third option is to set boundary conditions as

$$\mathbf{e}^T \underline{\mathbf{B}}^+ \mathbf{e} + \mathbf{e}_g^T \underline{\mathbf{B}}^- \mathbf{e}_g = \mathbf{e}^T (\underline{\mathbf{A}}^+ + \underline{\mathbf{E}}^{*,+}) \mathbf{e} + \mathbf{e}_g^T (\underline{\mathbf{A}}^- + \underline{\mathbf{E}}^{*,-}) \mathbf{e}_g. \quad (\text{A.6})$$

However the matrices $\underline{\mathbf{E}}^{*,\pm}$ are only related to $\underline{\mathbf{E}}$ through the eigenvalues and eigenvectors of $\underline{\mathbf{B}}$, making it more difficult to find the direct relation to errors in the boundary.

Appendix B. Derivation of Error Terms in 2D

Here we derive the error term $\mathcal{R} = -D1 - D2 + \gamma DG + V1 + V2 + V3 + V4$ in (89) in terms of the geometric errors (86) for the two dimensional domain of Fig. 2. Those error terms depend on $\nabla_\xi \varepsilon$. From (83),

$$\begin{aligned} \nabla_\xi \varepsilon &= \frac{\epsilon \nabla_\xi J - J \nabla_\xi \epsilon}{(J + \epsilon)^2} = \frac{\epsilon \nabla_\xi J - J \nabla_\xi \epsilon}{J^2(1 + \epsilon/J)^2} = \frac{\epsilon \nabla_\xi J - J \nabla_\xi \epsilon}{J^2} \left(1 - 2\frac{\epsilon}{J} + O(\epsilon^2)\right) \\ &= \frac{\epsilon(\nabla_\xi J + 2\nabla_\xi \epsilon) - J \nabla_\xi \epsilon}{J^2} + HOTs, \end{aligned} \quad (\text{B.1})$$

which needs $\nabla_\xi \epsilon$ and $\nabla_\xi J$.

First, from (86),

$$\begin{aligned} \frac{\partial \epsilon}{\partial \xi} &= \hat{z} \cdot \left\{ \left(\Delta \vec{\Gamma} \times \vec{X}_{\xi\xi} \right) + \left(\Delta \vec{\Gamma}' \times \vec{X}_\xi \right) + (1 - \eta) \left[\left(\Delta \vec{\Gamma}'' \times \vec{X}_\eta \right) + \left(\Delta \vec{\Gamma}' \times \vec{X}_{\eta\xi} \right) - \left(\Delta \vec{\Gamma}'' \times \Delta \vec{\Gamma} \right) \right] \right\} \\ &= \hat{z} \cdot \left\{ \left(\hat{\alpha} \times \vec{X}_{\xi\xi} \right) \left| \Delta \vec{\Gamma} \right| + \left(\hat{\beta} \times \vec{X}_\xi \right) \left| \Delta \vec{\Gamma}' \right| + (1 - \eta) \left[\left(\hat{\gamma} \times \vec{X}_\eta \right) \left| \Delta \vec{\Gamma}'' \right| + \left(\hat{\beta} \times \vec{X}_{\eta\xi} \right) \left| \Delta \vec{\Gamma}' \right| - \left(\hat{\gamma} \times \hat{\alpha} \right) \left| \Delta \vec{\Gamma} \right| \left| \Delta \vec{\Gamma}'' \right| \right] \right\} \\ &\equiv s_1 \left| \Delta \vec{\Gamma} \right| + (s_2 + (1 - \eta)s_4) \left| \Delta \vec{\Gamma}' \right| + (1 - \eta) \left[s_3 \left| \Delta \vec{\Gamma}'' \right| + s_5 \left| \Delta \vec{\Gamma} \right| \left| \Delta \vec{\Gamma}'' \right| \right], \end{aligned} \quad (\text{B.2})$$

where

$$s_1 = \hat{z} \cdot \left(\hat{\alpha} \times \vec{X}_{\xi\xi} \right), \quad s_2 = \hat{z} \cdot \left(\hat{\beta} \times \vec{X}_\xi \right), \quad s_3 = \hat{z} \cdot \left(\hat{\gamma} \times \vec{X}_\eta \right), \quad s_4 = \left(\hat{\beta} \times \vec{X}_{\eta\xi} \right), \quad s_5 = \hat{z} \cdot \left(\hat{\alpha} \times \hat{\gamma} \right).$$

Similarly,

$$\begin{aligned} \frac{\partial \epsilon}{\partial \eta} &= \hat{z} \cdot \left\{ \left(\hat{\alpha} \times \vec{X}_{\xi\eta} \right) \left| \Delta \vec{\Gamma} \right| - \left(\hat{\beta} \times \vec{X}_\eta \right) \left| \Delta \vec{\Gamma}' \right| + (1 - \eta) \left(\hat{\beta} \times \vec{X}_{\eta\eta} \right) \left| \Delta \vec{\Gamma}' \right| + \left(\hat{\beta} \times \hat{\alpha} \right) \left| \Delta \vec{\Gamma}' \right| \left| \Delta \vec{\Gamma} \right| \right\} \\ &\equiv p_1 \left| \Delta \vec{\Gamma} \right| - (p_2 - (1 - \eta)p_3) \left| \Delta \vec{\Gamma}' \right| + p_4 \left| \Delta \vec{\Gamma}' \right| \left| \Delta \vec{\Gamma} \right| \end{aligned} \quad (\text{B.3})$$

where

$$p_1 = \hat{z} \cdot \left(\hat{\alpha} \times \vec{X}_{\xi\eta} \right), \quad p_2 = \hat{z} \cdot \left(\hat{\beta} \times \vec{X}_\eta \right), \quad p_3 = \hat{z} \cdot \left(\hat{\beta} \times \vec{X}_{\eta\eta} \right), \quad p_4 = \hat{z} \cdot \left(\hat{\beta} \times \hat{\alpha} \right).$$

Then

$$\begin{aligned} J^2 \frac{\partial \varepsilon}{\partial \xi} &= \left(r_1 \left| \Delta \vec{\Gamma} \right| + (1 - \eta)r_2 \left| \Delta \vec{\Gamma}' \right| \right) \left(J_\xi + 2 \left(s_1 \left| \Delta \vec{\Gamma} \right| + (s_2 + (1 - \eta)s_4) \left| \Delta \vec{\Gamma}' \right| + (1 - \eta)s_3 \left| \Delta \vec{\Gamma}'' \right| \right) \right) \\ &\quad - J \left(s_1 \left| \Delta \vec{\Gamma} \right| + (s_2 + (1 - \eta)s_4) \left| \Delta \vec{\Gamma}' \right| + (1 - \eta)s_3 \left| \Delta \vec{\Gamma}'' \right| \right) + HOTs \\ &= (r_1 J_\xi - J s_1) \left| \Delta \vec{\Gamma} \right| + [(1 - \eta)r_2 J_\xi - J (s_2 + (1 - \eta)s_4)] \left| \Delta \vec{\Gamma}' \right| - J(1 - \eta)s_3 \left| \Delta \vec{\Gamma}'' \right| + HOTs \end{aligned} \quad (\text{B.4})$$

and

$$\begin{aligned} J^2 \frac{\partial \varepsilon}{\partial \eta} &= \left(r_1 \left| \Delta \vec{\Gamma} \right| + (1 - \eta)r_2 \left| \Delta \vec{\Gamma}' \right| \right) \left(J_\eta + 2 \left(p_1 \left| \Delta \vec{\Gamma} \right| - (p_2 - (1 - \eta)p_3) \left| \Delta \vec{\Gamma}' \right| \right) \right) \\ &\quad - J \left(p_1 \left| \Delta \vec{\Gamma} \right| - (p_2 - (1 - \eta)p_3) \left| \Delta \vec{\Gamma}' \right| \right) + HOTs \\ &= (r_1 J_\eta - J p_1) \left| \Delta \vec{\Gamma} \right| + ((1 - \eta)r_2 J_\eta + J (p_2 - (1 - \eta)p_3)) \left| \Delta \vec{\Gamma}' \right| + HOTs \end{aligned} \quad (\text{B.5})$$

where r_1, r_2, r_3 are defined in (87).

Again from (86), $\tilde{\mathbf{E}}^1 \propto |\Delta\vec{\Gamma}|$ and $\tilde{\mathbf{E}}^2 \propto |\Delta\vec{\Gamma}'|$. Therefore, as noted in the observations at the end of Sec. 5, $\tilde{\mathbf{E}} \cdot \nabla_\xi \varepsilon$, the functional that contributes to c_1 , has only higher order terms.

On the other hand, the contributor to c_2 is

$$\begin{aligned}
\tilde{\mathbf{A}} \cdot \nabla_\xi \varepsilon &= \frac{\tilde{\mathbf{A}}^1}{J^2} \left\{ (r_1 J_\xi - J s_1) |\Delta\vec{\Gamma}| + [(1-\eta)r_2 J_\xi - J(s_2 + (1-\eta)s_4)] |\Delta\vec{\Gamma}'| - J(1-\eta)s_3 |\Delta\vec{\Gamma}''| \right\} \\
&+ \frac{\tilde{\mathbf{A}}^2}{J^2} \left\{ (r_1 J_\eta - J p_1) |\Delta\vec{\Gamma}| + ((1-\eta)r_2 J_\eta + J(p_2 - (1-\eta)p_3)) |\Delta\vec{\Gamma}'| \right\} + HOTs \\
&= |\Delta\vec{\Gamma}| \left\{ \frac{\tilde{\mathbf{A}}^1}{J^2} (r_1 J_\xi - J s_1) + \frac{\tilde{\mathbf{A}}^2}{J^2} (r_1 J_\eta - J p_1) \right\} \\
&+ |\Delta\vec{\Gamma}'| \left\{ \frac{\tilde{\mathbf{A}}^1}{J^2} [(1-\eta)r_2 J_\xi - J(s_2 + (1-\eta)s_4)] + \frac{\tilde{\mathbf{A}}^2}{J^2} [(1-\eta)r_2 J_\eta + J(p_2 - (1-\eta)p_3)] \right\} \\
&- |\Delta\vec{\Gamma}''| \left\{ \frac{\tilde{\mathbf{A}}^1}{J} (1-\eta)s_3 \right\} + HOTs \\
&\equiv |\Delta\vec{\Gamma}| \underline{\mathbf{M}}_1 + |\Delta\vec{\Gamma}'| \underline{\mathbf{M}}_2 + |\Delta\vec{\Gamma}''| \underline{\mathbf{M}}_3 + HOTs,
\end{aligned} \tag{B.6}$$

where

$$\begin{aligned}
\underline{\mathbf{M}}_1 &= \frac{\tilde{\mathbf{A}}^1}{J^2} (r_1 J_\xi - J s_1) + \frac{\tilde{\mathbf{A}}^2}{J^2} (r_1 J_\eta - J p_1) \\
\underline{\mathbf{M}}_2 &= \frac{\tilde{\mathbf{A}}^1}{J^2} [(1-\eta)r_2 J_\xi - J(s_2 + (1-\eta)s_4)] + \frac{\tilde{\mathbf{A}}^2}{J^2} [(1-\eta)r_2 J_\eta + J(p_2 - (1-\eta)p_3)] \\
\underline{\mathbf{M}}_3 &= -\frac{\tilde{\mathbf{A}}^1}{J} (1-\eta)s_3.
\end{aligned} \tag{B.7}$$

Next,

$$\tilde{\mathbf{E}} \cdot \nabla_\xi \mathbf{q} = |\Delta\vec{\Gamma}| \hat{\mathbf{A}}_1 \mathbf{q}_\xi + |\Delta\vec{\Gamma}'| (1-\eta) \hat{\mathbf{A}}_2 \mathbf{q}_\eta \tag{B.8}$$

and

$$\varepsilon = -\frac{1}{J} \left\{ r_1 |\Delta\vec{\Gamma}| + (1-\eta)r_2 |\Delta\vec{\Gamma}'| \right\} + HOTs. \tag{B.9}$$

Then from (57),

$$\begin{aligned}
V2 &\leq \frac{1}{2} \left\{ \left| \left\langle |\Delta\vec{\Gamma}| \mathbf{e}, \underline{\mathbf{M}}_1 \mathbf{e} \right\rangle \right| + \left| \left\langle |\Delta\vec{\Gamma}'| \mathbf{e}, \underline{\mathbf{M}}_2 \mathbf{e} \right\rangle \right| + \left| \left\langle |\Delta\vec{\Gamma}''| \mathbf{e}, \underline{\mathbf{M}}_3 \mathbf{e} \right\rangle \right| + HOTs \right. \\
&\leq \left. \left\{ |\Delta\vec{\Gamma}|_{max} \left\| \frac{\underline{\mathbf{M}}_1}{J} \right\|_{2,\infty} + |\Delta\vec{\Gamma}'|_{max} \left\| \frac{\underline{\mathbf{M}}_2}{J} \right\|_{2,\infty} + |\Delta\vec{\Gamma}''|_{max} \left\| \frac{\underline{\mathbf{M}}_3}{J} \right\|_{2,\infty} \right\} \|\mathbf{e}\|_J^2 + HOTs.
\end{aligned} \tag{B.10}$$

Next, since $\varepsilon \tilde{\mathbf{E}}$ is of higher order,

$$\begin{aligned}
V3 &\leq \left| \left\langle |\Delta\vec{\Gamma}| \hat{\mathbf{A}}_1 \mathbf{q}_\xi, \mathbf{e} \right\rangle \right| + \left| \left\langle |\Delta\vec{\Gamma}'| (1-\eta) \hat{\mathbf{A}}_2 \mathbf{q}_\eta, \mathbf{e} \right\rangle \right| \\
&\leq |\Delta\vec{\Gamma}|_{max} \left\| \frac{\hat{\mathbf{A}}_1 \mathbf{q}_\xi}{J^2} \right\|_J \|\mathbf{e}\|_J + |\Delta\vec{\Gamma}'|_{max} \left\| \frac{(1-\eta) \hat{\mathbf{A}}_2 \mathbf{q}_\eta}{J^2} \right\|_J \|\mathbf{e}\|_J + HOTs.
\end{aligned} \tag{B.11}$$

Finally,

$$\begin{aligned}
V4 &= \left\langle \frac{1}{J} \left\{ r_1 |\Delta\vec{\Gamma}| + (1-\eta)r_2 |\Delta\vec{\Gamma}'| \right\} (\tilde{\mathbf{A}} \cdot \nabla_\xi \mathbf{q}), \mathbf{e} \right\rangle + HOTs \\
&= \left\langle \frac{1}{J^2} r_1 |\Delta\vec{\Gamma}| (\tilde{\mathbf{A}} \cdot \nabla_\xi \mathbf{q}), J\mathbf{e} \right\rangle + \left\langle \frac{1}{J^2} (1-\eta)r_2 |\Delta\vec{\Gamma}'| (\tilde{\mathbf{A}} \cdot \nabla_\xi \mathbf{q}), J\mathbf{e} \right\rangle + HOTs \\
&\leq |\Delta\vec{\Gamma}|_{max} \left\| \frac{r_1 (\tilde{\mathbf{A}} \cdot \nabla_\xi \mathbf{q})}{J^3} \right\|_J \|\mathbf{e}\|_J + |\Delta\vec{\Gamma}'|_{max} \left\| \frac{(1-\eta)r_2 (\tilde{\mathbf{A}} \cdot \nabla_\xi \mathbf{q})}{J^3} \right\|_J \|\mathbf{e}\|_J + HOTs.
\end{aligned} \tag{B.12}$$

The quantity $V1$ in (89) is of higher order in the Δ 's.

What remains is to find the dependencies of the boundary error terms in (89). The first two boundary terms represent dissipation error from waves exiting the domain. Along $\vec{\Gamma}_1^e$, $\eta = 0$, so with (B.9),

$$D1 = \int_0^1 \frac{1}{J} \left\{ r_1 \left| \Delta \vec{\Gamma} \right| + r_2 \left| \Delta \vec{\Gamma}' \right| \right\} \mathbf{e}^T \underline{\mathbf{A}}^+ \mathbf{e} d\xi + HOTs. \quad (\text{B.13})$$

Next, from (86),

$$\underline{\mathbf{E}}^\pm = \frac{1}{2} \left| \Delta \vec{\Gamma}' \right| \left\{ \hat{\mathbf{A}}_2 \pm \left| \hat{\mathbf{A}}_2 \right| \right\} = \left| \Delta \vec{\Gamma}' \right| \hat{\mathbf{A}}_2^\pm. \quad (\text{B.14})$$

The term $\varepsilon \underline{\mathbf{E}}^\pm$ is second order or higher, so,

$$D2 = \int_0^1 \left| \Delta \vec{\Gamma}' \right| \mathbf{e}^T \hat{\mathbf{A}}_2^+ \mathbf{e} d\xi + HOTs \quad (\text{B.15})$$

So to lowest order, the total outflow dissipation error is $O\left(\left| \Delta \vec{\Gamma} \right|, \left| \Delta \vec{\Gamma}' \right|\right)$.

The next boundary term in (89) is secondary, for it has quadratic dependence on $\left| \Delta \vec{\Gamma} \right|$,

$$DG = \int_0^1 \left| \Delta \vec{\Gamma} \right|^2 \left\{ (1 + \varepsilon) \hat{\alpha}^T \cdot \nabla_x \mathbf{g}^T \left\{ \left| \underline{\mathbf{A}}^- \right| + \left| \underline{\mathbf{E}}^- \right| \right\} \nabla_x \mathbf{g} \cdot \hat{\alpha} \Big|_{\eta=0} \right\} d\xi. \quad (\text{B.16})$$

When we account for the dissipation being positive and gather terms,

$$\begin{aligned} |\mathcal{R}(\Delta \vec{\Gamma}, \Delta \vec{\Gamma}', \Delta \vec{\Gamma}'')| &\leq \left| \Delta \vec{\Gamma} \right|_{max} \left\{ \frac{1}{2} \left\| \frac{\mathbf{M}_1}{J} \right\|_{2,\infty} \|\mathbf{e}\|_J + \left\| \frac{\hat{\mathbf{A}}_1 \mathbf{q} \xi}{J^2} \right\|_J + \left\| \frac{r_1 \left(\vec{\hat{\mathbf{A}}} \cdot \nabla_\xi \mathbf{q} \right)}{J^3} \right\|_J \right\} \|\mathbf{e}\|_J \\ &+ \left| \Delta \vec{\Gamma}' \right|_{max} \left\{ \frac{1}{2} \left\| \frac{\mathbf{M}_2}{J} \right\|_{2,\infty} \|\mathbf{e}\|_J + \left\| \frac{(1-\eta) \hat{\mathbf{A}}_2 \mathbf{q} \eta}{J^2} \right\|_J + \left\| \frac{(1-\eta) r_2 \left(\vec{\hat{\mathbf{A}}} \cdot \nabla_\xi \mathbf{q} \right)}{J^3} \right\|_J \right\} \|\mathbf{e}\|_J \\ &+ \left| \Delta \vec{\Gamma}'' \right|_{max} \left\{ \frac{1}{2} \left\| \frac{\mathbf{M}_3}{J} \right\|_{2,\infty} \|\mathbf{e}\|_J \right\} \|\mathbf{e}\|_J + HOTs, \end{aligned} \quad (\text{B.17})$$

so $\mathcal{R} = O\left(\left| \Delta \vec{\Gamma} \right|, \left| \Delta \vec{\Gamma}' \right|, \left| \Delta \vec{\Gamma}'' \right|\right)$.

References

- [1] J.-P. Ampuero, SEM2DPACK, A Spectral Element Method tool for 2D wave propagation and earthquake source dynamics, User's Guide, doi:10.5281/zenodo.230363, 2012.
- [2] C. Cantwell, D. Moxey, A. Comerford, A. Bolis, G. Rocco, G. Mengaldo, D. De Grazia, S. Yakovlev, J.-E. Lombard, D. Ekelschot, B. Jordi, H. Xu, Y. Mohamied, C. Eskilsson, B. Nelson, P. Vos, C. Biotto, R. Kirby, S. Sherwin, Nektar++: An open-source spectral/*hp* element framework, Computer Physics Communications 192 (2015) 205–219, doi:10.1016/j.cpc.2015.02.008.
- [3] N. Krais, A. Beck, T. Bolemann, H. Frank, D. Flad, G. Gassner, F. Hindenlang, M. Hoffmann, T. Kuhn, M. Sonntag, C.-D. Munz, FLEXI: A high order discontinuous Galerkin framework for hyperbolic–parabolic conservation laws, Computers & Mathematics with Applications 81 (2021) 186–219, doi:10.1016/j.camwa.2020.05.004.

- [4] M. Schlottke-Lakemper, A. R. Winters, H. Ranocha, G. J. Gassner, A purely hyperbolic discontinuous Galerkin approach for self-gravitating gas dynamics, *Journal of Computational Physics* 442 (2021) 110467, doi:10.1016/j.jcp.2021.110467.
- [5] L. Martire, R. Martin, Q. Brissaud, R. F. Garcia, SPECFEM2D-DG, an open-source software modelling mechanical waves in coupled solid–fluid systems: the linearized Navier–Stokes approach, *Geophysical Journal International* 228 (1) (2021) 664–697, doi:10.1093/gji/ggab308.
- [6] P. Fischer, S. Kerkemeier, M. Min, Y.-H. Lan, M. Phillips, T. Rathnayake, E. Merzari, A. Tomboulides, A. Karakus, N. Chalmers, T. Warburton, NekRS, a GPU-accelerated spectral element Navier–Stokes solver, *Parallel Computing* 114 (2022) 102982, doi:10.1016/j.parco.2022.102982.
- [7] E. Ferrer, G. Rubio, G. Ntoukas, W. Laskowski, O. Mariño, S. Colombo, A. Mateo-Gabín, H. Marbona, F. Manrique de Lara, D. Huergo, J. Manzanero, A. Rueda-Ramírez, D. Kopriva, E. Valero, HORSES3D: A high-order discontinuous Galerkin solver for flow simulations and multi-physics applications, *Computer Physics Communications* 287 (2023) 108700, doi:10.1016/j.cpc.2023.108700.
- [8] M. Kurz, D. Kempf, M. P. Blind, P. Kopper, P. Offenhäuser, A. Schwarz, S. Starr, J. Keim, A. Beck, GALÆXI: Solving complex compressible flows with high-order discontinuous Galerkin methods on accelerator-based systems, *Computer Physics Communications* 306 (2025) 109388, doi:https://doi.org/10.1016/j.cpc.2024.109388.
- [9] F. Hindenlang, Mesh Curving Techniques for High Order Parallel Simulations on Unstructured Meshes, Ph.D. thesis, University of Stuttgart, 2014.
- [10] T. Toulorge, J. Lambrechts, J.-F. Remacle, Optimizing the geometrical accuracy of curvilinear meshes, *Journal of Computational Physics* 310 (2016) 361–380, doi:10.1016/j.jcp.2016.01.023.
- [11] E. Ruiz-Gironés, J. Sarrate, X. Roca, Defining an 2-disparity Measure to Check and Improve the Geometric Accuracy of Non-interpolating Curved High-order Meshes, *Procedia Engineering* 124 (2015) 122–134, doi:10.1016/j.proeng.2015.10.127.
- [12] T. Bjøntegaard, E. M. Rønquist, Ø. Tråsdahl, Spectral Approximation of Partial Differential Equations in Highly Distorted Domains, *Journal Of Scientific Computing* 52 (3) (2012) 603–618, doi:10.1007/s10915-011-9561-8.
- [13] S. Sherwin, J. Peiró, Mesh generation in curvilinear domains using high-order elements, *International Journal for Numerical Methods in Engineering* 53 (1) (2002) 207–223, doi:10.1002/nme.397.
- [14] J. Nordström, S. Nikkar, Hyperbolic systems of equations posed on erroneous curved domains, *Journal of Computational Physics* 308 (2016) 438 – 442, doi:10.1016/j.jcp.2015.12.048.
- [15] S. Chun, J. Marcon, J. Peiró, S. J. Sherwin, Reducing errors caused by geometrical inaccuracy to solve partial differential equations with moving frames on curvilinear domain, *Computer Methods in Applied Mechanics and Engineering* 398 (2022) 115261, doi:https://doi.org/10.1016/j.cma.2022.115261.

- [16] G. J. Gassner, A. R. Winters, F. J. Hindenlang, D. A. Kopriva, The BR1 Scheme is Stable for the Compressible Navier–Stokes Equations, *Journal of Scientific Computing* 77 (1) (2018) 154–200, doi:10.1007/s10915-018-0702-1.
- [17] D. A. Kopriva, Metric identities and the discontinuous spectral element method on curvilinear meshes, *Journal of Scientific Computing* 26 (3) (2006) 301–327, doi:10.1007/s10915-005-9070-8.
- [18] J. Nordström, A Roadmap to Well Posed and Stable Problems in Computational Physics, *Journal Of Scientific Computing* 71 (1) (2017) 365–385, doi:10.1007/s10915-016-0303-9.
- [19] D. A. Kopriva, A. R. Winters, M. Schlottke-Lakemper, J. A. Schoonover, H. Ranocha, HOHQMesh: An All Quadrilateral/Hexahedral Unstructured Mesh Generator for High Order Elements, *Journal of Open Source Software* 9 (104) (2024) 7476, doi:10.21105/joss.07476.
- [20] F. Hindenlang, T. Bolemann, C. D. Munz, Mesh Curving Techniques for High Order Discontinuous Galerkin Simulations, in: N. Kroll, C. Hirsch, F. Bassi, C. Johnston, K. Hillewaert (Eds.), *IDI-HOM: Industrialization of High-Order Methods - A Top-Down Approach: Results of a Collaborative Research Project Funded by the European Union, 2010 - 2014*, Springer International Publishing, 133–152, doi:10.1007/978-3-319-12886-3_8, 2015.
- [21] J. Nordström, Error Bounded Schemes for Time-dependent Hyperbolic Problems, *SIAM Journal on Scientific Computing* 30 (1) (2008) 46–59, doi:10.1137/060654943.
- [22] W. Gordon, C. Hall, Construction of curvilinear co-ordinate systems and their applications to mesh generation, *International Journal for Numerical Methods in Engineering* 7 (1973) 461–477, doi:10.1002/nme.1620070405.
- [23] D. A. Kopriva, *Implementing Spectral Methods for Partial Differential Equations*, Scientific Computation, Springer, doi:10.1007/978-90-481-2261-5, 2009.